A Matheuristic for the Electric Vehicle Routing Problem with Capacitated Charging Stations

Aurélien Froger, Jorge E. Mendoza, Ola Jabali, Gilbert Laporte

CIRRELT

Centre interuniversitaire de recherche
sur les réseaux d'entreprise, la logistique et le transport

Interuniversity Research Centre
on Enterprise Networks, Logistics and Transportation

A Matheuristic for the Electric Vehicle Routing Problem with Capacitated Charging Stations

Aurélien Froger
Jorge E. Mendoza
Ola Jabali
Gilbert Laporte

June 2017

CIRRELT-2017-31

Bureaux de Montréal :
Université de Montréal
Pavillon André-Aisenstadt
C.P. 6128, succursale Centre-ville
Montréal (Québec)
Canada H3C 3J7
Téléphone : 514 343-7575
Télécopie : 514 343-7121

Bureaux de Québec :
Université Laval
Pavillon Palasis-Prince
2325, de la Terrasse, bureau 2642
Québec (Québec)
Canada G1V 0A6
Téléphone : 418 656-2073
Télécopie : 418 656-2624

www.cirrelt.ca

A Matheuristic for the Electric Vehicle Routing Problem with Capacitated Charging Stations

Aurélien Froger[1,2,*], Jorge E. Mendoza[2], Ola Jabali[3], Gilbert Laporte[1]

[1] Interuniversity Research Centre on Enterprise Networks, Logistics and Transportation (CIRRELT) and Department of Management Sciences, HEC Montréal, 3000 Côte-Sainte-Catherine, Montréal, Canada H3T 2A7

[2] Université François-Rabelais de Tours, LI EA 6300, ROOT ERL CNRS 6305, Tours, France

[3] Dipartimento di Elettronica, Informazione e Bioingegneria, Politecnico di Milano, Piazza Leonardo da Vinci, 32, Milano 20133, Italy

Abstract. Existing research on Electric vehicle routing problems (E-VRPs) assumes that charging stations (CSs) can simultaneously charge an unlimited number of electric vehicles. In practice, however, CSs have a limited number of chargers. In this research, we investigate the impact of considering these capacity restrictions. We focus on the electric vehicle routing problem with nonlinear charging function (E-VRP-NL). We first extend existing mixed integer linear programming formulations of the E-VRP-NL to deal with capacitated CSs. We then present a route-first assemble-second matheuristic to tackle the problem. In the first stage of this method, we rely on an existing metaheuristic to generate a pool of high-quality routes while relaxing the capacity constraints. In the second stage, we use a Benders' like decomposition to assemble a solution to the problem by assembling routes from the pool. We evaluate four different assembling strategies. The results suggest that our algorithm performs well on a set of instances adapted from the literature.

Keywords: Electric vehicle routing problem with nonlinear charging function, mixed integer linear programming, benders decomposition, matheuristic.

Acknowledgements. This research was partly funded in France by Agence Nationale de la Recherche through project e-VRO (ANR-15-CE22-0005-01).

---

* Corresponding author: Aurelien.Froger@cirrelt.ca

Dépôt légal – Bibliothèque et Archives nationales du Québec
Bibliothèque et Archives Canada, 2017

1. Introduction and motivation

Electric vehicle routing problems (E-VRPs) started to be studied by the Operational Research (OR) community only recently. They consist in designing routes to serve a set of customers using a fleet of electric vehicles (EVs). Due to their relatively short driving range the EVs can detour to charging stations (CSs) to replenish their battery. Decisions in E-VRPs concern not only the sequence in which the customers are to be served, but also where and how much to charge the batteries. It is safe to say that one of the key elements in E-VRPs is the modeling of the charging process. For instance, some studies assume that the vehicle is fully replenished whenever they detour to a CS. In the green vehicle routing problem (G-VRP) tackled by Erdoğan and Miller-Hooks (2012), Koč and Karaoglan (2016), Montoya et al. (2016), andBartolini and Andelmin (2017), charging an EV is done in constant time, while in (Schneider et al., 2014), (Hiermann et al., 2016), (Keskin and Čatay, 2016), and (Desaulniers et al., 2016) the charging time linearly depends on the state of charge (SoC) of the EV at its arrival at the CS. The full charging policy may be too restrictive. To overcome its drawbacks and to potentially save energy and time, one possibility is to allow partial recharge. This policy has been investigated in (Bruglieri et al., 2015), (Desaulniers et al., 2016), (Felipe et al., 2014), (Montoya et al., 2017), and (Froger et al., 2017). The latter three have studied the case in which, like in practice, CSs may have different technologies. Additionally, to account for the nonlinear relation between the time spent charging and the amount of energy charged, Montoya et al. (2017) and Froger et al. (2017) modeled charging functions using piecewise linear expressions. This results in the definition of the electric vehicle routing problem with nonlinear charging function (E-VRP-NL).

It is noteworthy that the above-mentioned assume that the charging infrastructure is private, that is, that the CSs are always available. This is a plausible assumption, since large companies can decide to invest in their own Infrastructure to avoid dealing with the uncertainty in CSs availability (e.g, queues). However, to the best of our knowledge, one of the key assumptions in the E-VRPs defined in the literature is that the CSs are uncapacitated, that is, they are able to simultaneously handle an unlimited number of EVs. In practice, however, each CS has a limited number of chargers which limits the number of EVs charging at the same time. Needless to say, neglecting the CS capacity constraints may lead to poor decisions in practice. For instance we ran a feasibility test on the 120 BKS for the E-VRP-NL reported in (Montoya et al., 2017) limiting the number of chargers per CS to 1, 2, 3, and 4. According to our results, nearly 50% of the Montoya et al. (2017) solutions become infeasible when only 1 charger is available. This figure drops to 11% and 2% for the cases with 2 and 3 chargers. On the other hand, when 4 chargers are available, all solutions remain feasible. It is worth noting that if a company decides to invest in out-of-the-depot charging infrastructure, there are few chances that they decide to install more than a couple of chargers at each CS. AppendixA presents the details of our feasibility test.

In this research we focus on the E-VRP-NL and we extend it to consider capacitated CSs. We call the resulting problem the E-VRP-NL with capacitated CSs (E-VRP-NL-C). We first propose several modeling alternatives for the E-VRP-NL-C built on top of existing

MILP formulations of the E-VRP-NL. Then, we present a two-stage matheuristic to tackle the problem. The first stage of the algorithm consists in building a pool of routes while not taking the capacity constraints into account. The second stage of the algorithm assembles the routes from the pool to build a solution to the E-VRP-NL-C. We propose different strategies based on a Benders' like decomposition of the assembling problem. More specifically, the overall scheme of the approach consists in solving a set partitioning model and discarding, by means of cuts, all along the branch-and-bound tree, selections of routes that are infeasible or for which the total time is underestimated.

The remainder of this document is organized as follows. Section 2 formally introduces the E-VRP-NL-C. Section 3 describes MILP formulations of the problem. Section 4 presents a two-stage matheuristic approach to tackle the E-VRP-NL-C. Section 5 shows the computational results of our carried out experiments. Finally, Section 6 concludes and outlines research perspectives.

2. Problem description

We define the electric vehicle routing problem with nonlinear charging function and capacitated stations (E-VRP-NL-C) as follows.

Let I be the set of customers that need to be served and F the set of charging stations (CSs) at which the vehicles can stop to recharge their battery. Each customer $i \in I$ has a service time g_i. The customers are served using an unlimited and homogeneous fleet of EVs. The vehicle driving-range is limited by a route duration limit T_{max}. All the EVs have a battery of capacity Q (expressed in kWh). At the beginning of the planning horizon, the EVs are located in a single depot that they leave fully charged. Traveling from one location i (the depot, a customer, or a CS) to another location j incurs a driving time $t_{ij} \geqslant 0$ and an energy consumption $e_{ij} \geqslant 0$. Driving times and energy consumption both satisfy the triangular inequality. Due to their limited battery capacity, EVs may require to stop en route at CSs. Charging operations can occur at any CS and EVs can be partially recharged. Each CS $i \in F$ has a *capacity*, given by the number C_i of available chargers. Each CS has also a piecewise linear charging function $\Phi_i(\Delta)$ that maps for an empty battery the time Δ spent charging at i to the SoC of the vehicle when it leaves i. If q is the SoC of the EV when it arrives at i and Δ the charging time, the SoC of the EV when it departs from i is given by $\Phi_i(\Delta + \Phi_i^{-1}(q))$. We denote as $B_i = \{0, \ldots, b_i\}$ the set of breakpoints of the charging function at i (sorted in ascending order). We also introduce c_{ik} and a_{ik} to represent the charging time and the SoC for breakpoint $k \in B_i$ of the CS i. For notational convenience, let ρ_{ik} denote the slope of the segment between $c_{i,k-1}$ and c_{ik} (i.e. $\rho_{ik} = (a_{ik} - a_{i,k-1})/(c_{ik} - c_{i,k-1})$) and η_{ik} the y-intercept of the segment between $c_{i,k-1}$ and c_{ik} (i.e. $\eta_{ik} = a_{ik} - c_{ik}\rho_{ik}$).

Feasible solutions to the E-VRP-NL-C satisfy the following conditions:

1. each customer is visited exactly once by a single vehicl;
2. each route starts and ends at the depot
3. each route satisfies the maximum-duration limit T_{max}
4. each route is energy-feasible (i.e., the SoC of an EV when it arrives at and departs from any location is between 0 and Q)

5. no more than C_i EVs simultaneously charge at each CS $i \in F$

The objective of the E-VRP-NL-C is to minimize the total time. The latter takes into account driving, service, and charging times. Due to the limited availability of CSs, it also includes the waiting times that may occur at CSs whenever an EV queues for a charger.

3. Mixed-integer linear programming formulations

In this section we extend the formulations propose in (Froger et al., 2017) for the closely-related E-VRP-NL to deal with CS capacity constraints. Their formulations belong to two different families: CS replication-based formulations and recharging path-based formulations. The former share the spirit of the MILP formulations that are most typically used in the E-VRP literature. The latter, on the other hand, correspond to an alternative modeling strategy. According to their results recharging path-based formulations outperform CS replication-based formulations. We, however, decided to explore both types of formulations for the E-VRP-NL-C.

3.1. CS replication-based formulation

Similarly to the E-VRP-NL, the E-VRP-NL-C can be defined on a digraph $G = (V, A)$, where $V = \{0\} \cup I \cup F'$ is the set of nodes and A is the set of arcs connecting nodes of V. The symbol 0 represents the depot. The set F' contains β_i copies of each CS $i \in F$ (i.e., $|F'| = \sum_{i \in F} \beta_i$). The value of β_i corresponds to an upper bound on the number of visits to CS i. Note that β_i must be strictly greater than C_i; otherwise, the capacity constraints are redundant. In the remainder of this manuscript, depending on the context, we refer to an element of F' or F'_i as a CS copy or as a charging operation. We denote as $F'_i \subseteq F'$ the set containing the β_i copies of CS i (i.e., $|F'_i| = \beta_i$ and $F' = \bigcup_{i \in F} F'_i$). We assume that F'_i is an ordered set and that its elements are numbered from 1 to β_i. We use the preprocessing technique presented in (Froger et al., 2017) to reduce the number of arcs in A. In a nutshell, this technique primarily removes arcs that can never been traveled as regards to the battery capacity.

3.1.1. The baseline model

According to the experiments carried out in (Froger et al., 2017), the best formulations of the E-VRP-NL use arc-based tracking variables for the SoC and the time. Binary variable x_{ij} is 1 if and only if an EV travels arc $(i, j) \in A$. Continuous variables τ_{ij} and y_{ij} track (respectively) the time and SoC of an EV when it departs from vertex $i \in V$ to travel arc (i, j). If no vehicle travels between nodes i and j, both variables are 0. Continuous variables q_i and o_i specify (according to the piecewise linear approximation of the charging function) the SoC of an EV when it arrives at and departs from CS copy $i \in F'$. Continuous variable Δ_i represents the duration of the charging operation performed at CS copy $i \in F'$. Let $i \in F'$ be a CS copy and $k \in B_i \backslash \{0\}$. We introduce the continuous variable ϕ_{ik} representing the amount of energy charged at i on the segment that lies between the points $(c_{i,k-1}, a_{i,k-1})$ and (c_{ik}, a_{ik}). We also introduce the binary variable ω_{ik} taking the value of 1 if and only if an EV charges at i on the segment between the points $(c_{i,k-1}, a_{i,k-1})$ and (c_{ik}, a_{ik}). In the

E-VRP-NL, optimal solutions are *left-shifted schedules*. Indeed, when minimizing the total time, there is no advantage to wait before serving any customer or before charging at any CS. In the E-VRP-NL-C, this does not hold since there are coupling constraints between the routes. As a matter of fact, it may sometimes be profitable to wait at a CS for an available charger rather than to go to another CS. Without loss of generality, we restrict waiting times to occur only before charging operations. We introduce a continuous variable ∇_i representing the waiting time of an EV before the start of the charging operation $i \in F'$. By adapting the existing CS replication-based formulations of the E-VRP-NL, a baseline model of the E-VRP-NL-C denoted as $[F^{CS}]$, is written as follows:

$$[F^{CS}] \min \sum_{i,j \in V} t_{ij} x_{ij} + \sum_{i \in F'} (\Delta_i + K \nabla_i) + \sum_{i \in I} g_i \tag{1}$$

subject to

$$\sum_{(i,j) \in A} x_{ij} = 1, \qquad \forall i \in I \tag{2}$$

$$\sum_{(i,j) \in A} x_{ij} \leqslant 1, \qquad \forall i \in F' \tag{3}$$

$$\sum_{(j,i) \in A} x_{ji} - \sum_{(i,j) \in A} x_{ij} = 0, \qquad \forall i \in V \tag{4}$$

$$\sum_{(i,j) \in A} (y_{ij} - e_{ij} x_{ij}) = \sum_{(j,l) \in A} y_{jl}, \qquad \forall j \in I \tag{5}$$

$$\sum_{(i,j) \in A} (y_{ij} - e_{ij} x_{ij}) = q_j, \qquad \forall j \in F' \tag{6}$$

$$\sum_{(j,l) \in A} y_{jl} = o_j, \qquad \forall j \in F' \tag{7}$$

$$y_{ij} \leqslant \left(Q - \min_{l \in F \cup \{0\}} e_{li} \right) x_{ij}, \qquad \forall (i,j) \in A \tag{8}$$

$$y_{ij} \geqslant \left(e_{ij} + \min_{l \in F \cup 0} e_{jl} \right) x_{ij}, \qquad \forall (i,j) \in A \tag{9}$$

$$q_i + \phi_{ik} \leqslant a_{ik} \omega_{ik} + Q(1 - \omega_{ik}), \qquad \forall i \in F', \forall k \in B_i \backslash \{0\} \tag{10}$$

$$\phi_{ik} \leqslant (a_{ik} - a_{i,k-1}) \omega_{ik}, \qquad \forall i \in F', \forall k \in B_i \backslash \{0\} \tag{11}$$

$$\sum_{k \in B_i \backslash \{0\}} \omega_{ik} \geqslant \sum_{(i,j) \in A} x_{ij}, \qquad \forall i \in F' \tag{12}$$

$$\omega_{ik} \leqslant \sum_{(i,j) \in A} x_{ij}, \qquad \forall i \in F', \forall k \in B_i \backslash \{0\} \tag{13}$$

$$o_i = q_i + \sum_{k \in B_i \backslash \{0\}} \phi_{ik}, \qquad \forall i \in F' \tag{14}$$

$$\Delta_i = \sum_{k \in B_i \backslash \{0\}} \phi_{ik} / \rho_{ik}, \qquad \forall i \in F' \tag{15}$$

$$\sum_{(i,j) \in A, i \neq 0} (\tau_{ij} + (t_{ij} + p_j) x_{ij}) = \sum_{(j,l) \in A} \tau_{jl}, \qquad \forall j \in I \tag{16}$$

$$\sum_{(i,j) \in A : i \neq 0} (\tau_{ij} + t_{ij} x_{ij}) + \Delta_j + \nabla_j = \sum_{(j,l) \in A} \tau_{jl}, \qquad \forall j \in F' \tag{17}$$

$$\tau_{ij} \leqslant (T_{max} - t_{ij} - p_j - t_{j0})\, x_{ij}, \qquad \forall (i,j) \in A : i \neq 0, j \in I \tag{18}$$

$$\tau_{ij} \leqslant \left(T_{max} - t_{ij} - \Delta_j^{min} - t_{j0}\right) x_{ij}, \qquad \forall (i,j) \in A : i \neq 0, j \in F' \tag{19}$$

$$\sum_{(h,j)\in A} x_{hj} \leqslant \sum_{(h,l)\in A} x_{hl}, \qquad \forall i \in F, \forall j,l \in F'_i, j < l \tag{20}$$

$$\sum_{(j,h)\in A: j\neq 0} \tau_{jh} - \Delta_j \geqslant \sum_{(l,h)\in A: l\neq 0} \tau_{lh} - \Delta_l, \qquad \forall i \in F, \forall j,h \in F'_i : j < l \tag{21}$$

$$x_{ij} \in \{0,1\}, \qquad \forall (i,j) \in A \tag{22}$$

$$\tau_{ij} \geqslant 0, \qquad \forall (i,j) \in A : i \neq 0 \tag{23}$$

$$y_{ij} \geqslant 0, \qquad \forall (i,j) \in A \tag{24}$$

$$q_i \geqslant 0, o_i \geqslant 0, \Delta_i \geqslant 0, \qquad \forall i \in F' \tag{25}$$

$$\phi_{ik} \geqslant 0 \qquad \forall i \in F', \forall k \in B_i \backslash \{0\} \tag{26}$$

$$\omega_{ik} \in \{0,1\} \qquad \forall i \in F', \forall k \in B_i \backslash \{0\} \tag{27}$$

Equation (1) gives the objective of the problem. It includes the driving, service, and charging times, but also a weighted sum (with a parameter $K > 0$) of the waiting times. Constraints (2) ensure that each customer is visited once. Constraints 3 ensure that each CS copy is visited at most once. Constraints (4) impose the flow conservation. Constraints (5) track the battery level at each customer. Constraints (6) track the battery level of the EV when it arrives at a CS copy. Constraints (7) track the battery level of the EV when it leaves a CS copy. Constraints (8) couple the y_{ij} and x_{ij} variables. Constraints (9) state that if an EV traverses the arc (i,j) its SoC when leaving i must be enough to traverse the arc and then to reach the closest CS or the depot. Constraints (10) restrict the segments on which EVs can charge according to the state of charge they have at their arrival at CS copies. Constraints (11) restrict the charging amount that can be charged on each segment. Constraints (12) impose the activation of one segment whenever an EV visits a CS copy. Constraints (13) are valid inequalities. Constraints (14) define the state of charge after a charging operation. Constraints (15) define the time spent charging at each CS copy. Constraints (16) track the departure time at each customer. Constraints (17) track the departure time at CS copies. Constraints (18) and (19) couple the τ_{ij} and x_{ij} variables. Specifically, if an EV traverses an arc (i,j), then its departure time must guarantee that the EV returns to the depot without exceeding the tour duration limit. Constraints (20) and (21) break symmetries created by the introduction of CS copies. These constraints ensure that the copies of CS i are visited in the reverse order they appear in F_i (i.e, a charging operation $j \in F'_i$ must start after a charging operation $l \in F'_i$ if $l > j$). The reverse order is used since departure time and charging duration variables take the value 0 when a CS copy is not visited. Finally, constraints (22)–(27) define the domain of the decision variables.

The E-VRP-NL-C is a combined routing (the EVs visiting customers) + scheduling (the charging operations) problem. To extend previous formulations of the E-VRP-NL to include the CS capacity constraints, we borrowed some ideas from the Resource Constrained Scheduling Problem (RCPSP) literature. More precisely, we propose two formulations, a *flow-based* and an *event-based*, drawing some inspiration from the models introduced by

Artigues et al. (2003) and Koné et al. (2011) for the RCPSP. There is, however, a major difference between our CS scheduling problem and the RCPSP or the related parallel machine scheduling problem: in our problem i) the duration of each task (i.e., charging operation) and ii) the number of tasks executed by each resource (i.e., charging station) are decision variables (they are problem parameters in the RCPSP). To the best of our knowledge this case has never been addressed in the literature before.

3.1.2. Flow-based modeling of the capacity constraints

In our flow-based formulation (hereafter referred to as FB), we consider C_i parallel machines for each CS $i \in F$. Each machine can execute at any given time at most one job. Let $i \in F$ be a CS and 0_i and $\beta_i + 1$ be two dummy charging operations (acting as the source and the sink of the flow). We denote as $\widetilde{F'}_i$ the set $F'_i \cup \{0_i, \beta_i + 1\}$ of charging operations (CS copies are here considered as charging operations). Without loss of generality, we can enforce that in any feasible solution, after the completion of an operation $j \in \widetilde{F'}_i$, the resource unit (charger) allocated to j is directly transferred to a unique operation $l \in \widetilde{F'}_i$.

The FB formulation requires the following decision variables. Sequential binary variable u_{jl} is equal to 1 if and only if charging operation l starts after the completion of charging operation $j > l$ (symmetry breaking constraints (21) impose that charging operation j starts before charging operation $l < j$). Let now $j, l \in \widetilde{F'}_i$ be two charging operations (potentially dummy) such that $j > l$. Continuous flow variable f_{jl} denotes the quantity of resource that is transferred from charging operation j to charging operation l. For notational convenience, we define $\widetilde{C}_j := 1$ for all $j \in F'_i$ and $\widetilde{C}_{0_i} := \widetilde{C}_{\beta_i+1} := C_i$.

For the sake of clarity, we provide here one example to illustrate the structure of the flow network. We consider in this example a CS i with 2 chargers (i.e. $C_i = 2$) and we create 4 copies of the CS ($\beta_i = 4$). Figure 1 shows an example of four charging operations occurring at this CS (hereafter referred to as Example 1). Figure 2 illustrates the structure of the flow network on this example and describes a feasible flow.

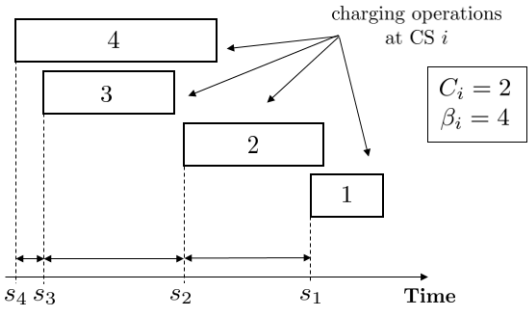

Figure 1: Charging operations at CS $i \in F$

A flow-based formulation of the capacity constraints is as follows:

$$\sum_{l \in \widetilde{F'}_i, l > j} f_{lj} = \sum_{(l,j) \in A} x_{lj} \qquad \forall i \in F, \forall j \in F'_i \tag{28}$$

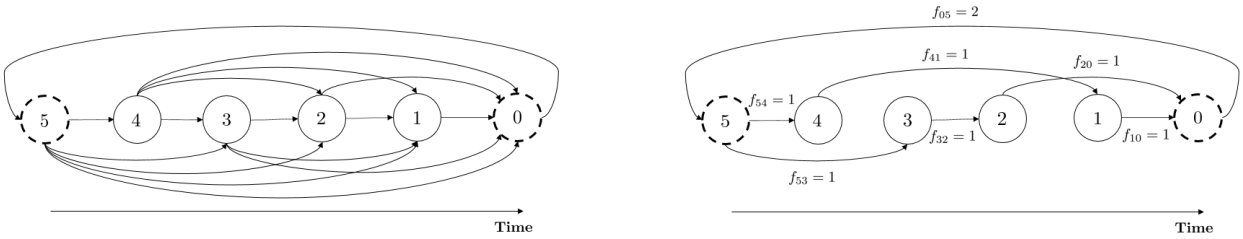

Figure 2: Structure of the flow network for CS i (left) and a feasible flow (right)

$$\sum_{l \in \widetilde{F'}_i, l > j} f_{lj} - \sum_{l \in \widetilde{F'}_i, l < j} f_{jl} = 0, \qquad \forall i \in F, \forall j \in F'_i \tag{29}$$

$$C_i - \sum_{l \in \widetilde{F'}_i, l > 0_i} f_{l,0_i} = 0, \qquad \forall i \in F \tag{30}$$

$$\sum_{l \in \widetilde{F'}_i, l < \beta_i + 1} f_{\beta_i + 1, l} - C_i = 0, \qquad \forall i \in F \tag{31}$$

$$u_{jh} \geqslant u_{jl} + u_{lh} - 1, \qquad \forall i \in F, \forall j, l, h \in F'_i : j > l > h \tag{32}$$

$$\sum_{(l,h) \in A} \tau_{lh} - \Delta_l - \sum_{(j,h) \in A} \tau_{jh} \geqslant (T_{max} - t_{i0})(u_{jl} - 1), \qquad \forall i \in F, \forall j, l \in F'_i, j > l \tag{33}$$

$$f_{jl} \leqslant \min(\widetilde{C}_j, \widetilde{C}_l) u_{jl}, \qquad \forall i \in F, \forall (j,l) \in F'_i, j > l \tag{34}$$

$$u_{jl} \in \{0, 1\}, \qquad \forall i \in F, \forall j, l \in F'_i, j > l \tag{35}$$

$$f_{jl} \geqslant 0 \qquad \forall i \in F, \forall j, l \in \widetilde{F'}_i, j > l \tag{36}$$

Constraints (28) state that a resource has to be allocated to a charging operation in F'_i if an EV reaches the corresponding CS. Constraints (29)-(31) ensure the flow conservation. Constraints (32) express the transitivity of the precedence relations. Constraints (33) are the disjunctive constraints coupling the start time of j and l to u_{jl}. The constraint is active when $u_{jl} = 1$ and, in that case, it enforces the precedence relation between the charging operations j and l (i.e., l cannot start before the completion of j). Constraints (34) couple the flow variables to the sequence variables. Constraints (35) and (36) define the domain of the decision variables.

3.1.3. Event-based formulation of the capacity constraints

This event-based formulation (hereafter referred to as EB) is inspired by the *on/off event-based formulation* introduced by Koné et al. (2011). Consider the start of a charging operation as an event. The intuition behind the EB formulation is to count the number of events that overlap with the execution of other charging operations and set a constraint on that number.

Similarly to the FB formulation, on the EB formulation we can write the CS capacity constraints independently for each CS i. We define binary variable v_{jl} that is 1 if and only if the charging operation at $j \in F'_i$ starts at the same time as charging operation $l \in F'_i$ ($j \geqslant l$) or is still being processed after the start of l. We use the variables $(v_{jl})_{j \in F'_i : j \geqslant l}$ to count the number of chargers required during each time interval defined by the starting time

of a charging operation j and $j-1$. Figure 3 illustrates the definition of these variables for Example 1.

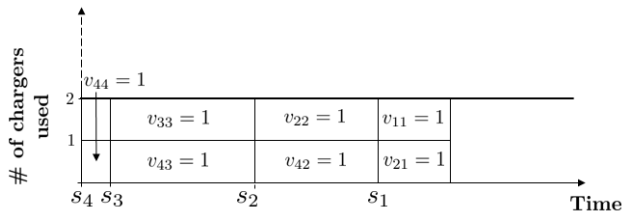

Figure 3: Illustration of the definition of variables $(v_{jl})_{j\in F_i':j\leqslant l}$ for CS i

An event-based formulation of the capacity constraints is as follows:

$$v_{jj} = \sum_{(h,j)\in A} x_{hj}, \qquad \forall i \in F, \forall j \in F_i' \tag{37}$$

$$\sum_{(l,h)\in A} \tau_{lh} - \Delta_l \geqslant \sum_{(j,h)\in A} \tau_{jh} - (1 + v_{jl} - v_{j,l+1})\,(T_{max} - t_{i0}) \qquad \forall i \in F, \forall j,l \in F_i' : j > l \tag{38}$$

$$\sum_{h=0}^{j-1} v_{jh} \leqslant j(1 - v_{j,l+1} + v_{jl}) \qquad \forall i \in F, \forall j,l \in F_i' : j > l \tag{39}$$

$$\sum_{j\in F_i':j\geqslant l} v_{jl} \leqslant C_i \qquad \forall i \in F, \forall l \in F_i' \tag{40}$$

$$v_{jl} \in \{0,1\}, \qquad \forall i \in F, \forall j,l \in F_i' : j \geqslant l \tag{41}$$

Constraints (37) forces each charging operation $j \in F_i'$ to activate variable v_{jj}. Constraints (38) ensure that if charging operation j ends before charging operation l starts, then the starting time of l is larger than the completion time of j. Constraints (39) enforce contiguity for the value of the v_{jl} variables. Since charging operations are non-preemptive, we can safely forbid cases where for $j \in F'$ there exists $l \in F_i'$ such that $v_{jl} = 1$, $v_{j,l-1} = 0$, and $v_{j,l-2} = 1$. Constraints (40) limit the number of charging operations that can be simultaneously performed. Constraints (41) define the domain of the newly introduced decision variables.

3.2. Recharging path-based formulation

One drawback of the previous formulations is the need to replicate the CSs. If we want to ensure that no optimal solutions are cut off, the number of copies to create has to be large. However this yields impracticable MILPs. See (Froger et al., 2017) for a detailed discussion on this issue. To overcome this difficulty, Froger et al. (2017) propose an alternative modeling of the E-VRP-NL-C based on the concept of recharging paths (hereafter sometimes referred to simply as paths) between each couple of nodes (either customers or the depot).

The concept of recharging paths leads to the definition of the E-VRP-NL-C on a directed multigraph $\widetilde{G} = (\widetilde{V}, \widetilde{A})$, where $\widetilde{V} = \{0\} \cup I$ and $\widetilde{A}$ is the set of arcs associated with paths connecting nodes of $\widetilde{V}$. Without preprocessing, the number of paths explodes with the

number of CSs and the number of customers. However, a large number of these arcs cannot be part of an optimal solution. A dominance rule can be applied to discard unpromising recharging paths. To find all the non-dominated paths, we use the procedure described in AppendixB. Let $i, j \in \widetilde{V}$ be two nodes such that $i \neq j$. We define P_{ij} as the set of (non-dominated) recharging paths connecting node i to node j by visiting none or some CSs. Let P be the set of all recharging paths connecting any couple of nodes in the graph. Specifically, we have $P = \bigcup_{i,j \in \widetilde{V}, i \neq j} P_{ij}$. We denote $o(p)$ and $d(p)$ as the origin and destination of a path $p \in P$. For each path p, we define an arc in $\widetilde{A}$ from $o(p)$ to $d(p)$. Let us denote n_p as the number of CSs in path p and let $L_p = \{0, 1..., n_p - 1\} \subset \mathbb{N}$ be the set of CS positions in the path p. Let $i(p, l)$ be the CS at position $l \in L_p$ in path p. Additionally, if an EV can travel from i to j without visiting any CS, we create the corresponding path (denoted p^0_{ij}) and add it to P_{ij}.

A recharging path-based formulation of the E-VRP-NL-C involves the following decisions variables. Binary variable x_p is 1 if and only if an EV travels recharging path $p \in P$. Continuous variables τ_p and y_p track the time and SoC of an EV when it departs from node $o(p)$ to $d(p)$ using path p. Continuous variables q_{pl} and o_{pl} specify (according to the piecewise linear approximation of the charging function) the SoC of an EV when it arrives at and departs from $i(p, l)$ (i.e. the CS at position $l \in L_p$). Continuous variable Δ_{pl} represent the duration of the charging operation performed at $i(p, l)$. Continuous variable ϕ_{plk} represents the amount of energy charged on the segment that lies between the points $(c_{i(p,l),k-1}, a_{i(p,l),k-1})$ and $(c_{i(p,l),k}, a_{i(p,l),k})$ at the CS $i(p, l)$. Binary variables ω_{plk} equal to one if and only if an EV charges at the CS at position l in path p on the segment between the points $(c_{i(p,l),k-1}, a_{i(p,l),k-1})$ and $(c_{i(p,l),k}, a_{i(p,l),k})$. Let e^p and t^p be the energy consumption and the driving time associated with path $p \in P$. Continuous variable ∇_{pl} represents the waiting time at the CS at position l in path p before charging. We also introduce starting and completion time for the charging operations. Continuous variables s_{pl} and d_{pl} represent the starting and completion time of the charging operation performed at $i(p, l)$.

A path-based formulation of the E-VRP-NL-C, denoted as $[P^{path}]$, is as follows:

$$[F^{path}] \quad \min \sum_{p \in P} \left(t^p x_p + \sum_{l \in L_p} (\Delta_{pl} + \nabla_{pl}) \right) + \sum_{i \in I} g_i \tag{42}$$

subject to

$$\sum_{j \in \widetilde{V}, i \neq j} \sum_{p \in P_{ij}} x_p = 1, \quad \forall i \in I \tag{43}$$

$$\sum_{j \in \widetilde{V}, i \neq j} \sum_{p \in P_{ji}} x_p - \sum_{j \in \widetilde{V}, i \neq j} \sum_{p \in P_{ij}} x_p = 0, \quad \forall i \in \widetilde{V} \tag{44}$$

$$\sum_{l \in \widetilde{V}, l \neq j} \sum_{p \in P_{lj}} \left(y_p - e^p x_p + \sum_{l \in L_p} (o_{pl} - q_{pl}) \right) = \sum_{l \in \widetilde{V}, l \neq j} \sum_{p \in P_{jl}} y_p, \quad \forall j \in I \tag{45}$$

$$y_p - e_{o(p),i(p,0)} x_p = q_{p0}, \quad \forall p \in P \tag{46}$$

$$o_{p,l-1} - e_{i(p,l-1),i(p,l)} x_p = q_{pl}, \quad \forall p \in P, \forall l \in L_p \backslash \{0\} \tag{47}$$

$$\sum_{i\in\tilde{V},i\neq 0}\sum_{p\in P_{i0}}\left(y_p - e^p x_p - \sum_{l\in L_p}(o_{pl}-q_{pl})\right)\geqslant 0,\quad \forall i\in I \tag{48}$$

$$y_p \leqslant Q x_p,\quad \forall p\in P \tag{49}$$

$$q_{pl}+\phi_{plk}\leqslant a_{i(p,l),k}\omega_{plk}+Q(1-\omega_{plk}),\quad \forall p\in P,\forall l\in L_p,\forall k\in B_{i(p,l)}\backslash\{0\} \tag{50}$$

$$\phi_{plk}\leqslant (a_{i(p,l),k}-a_{i(p,l),k-1})\omega_{plk},\quad \forall p\in P,\forall l\in L_p,\forall k\in B_{i(p,l)}\backslash\{0\} \tag{51}$$

$$\sum_{k\in B_{i(p,l)}\backslash\{0\}}\omega_{plk}\geqslant x_p,\quad \forall p\in P,\forall l\in L_p \tag{52}$$

$$\omega_{plk}\leqslant x_p,\quad \forall p\in P,\forall l\in L_p,\forall k\in B_{i(p,l)}\backslash\{0\} \tag{53}$$

$$o_{pl}=q_{pl}+\sum_{k\in B_{i(p,l)}\backslash\{0\}}\phi_{plk},\quad \forall p\in P,\forall l\in L_p \tag{54}$$

$$\Delta_{pl}=\sum_{k\in B_{i(p,l)}\backslash\{0\}}\phi_{plk}/\rho_{i_l k},\quad \forall p\in P,\forall l\in L_p \tag{55}$$

$$\sum_{i\in\tilde{V}\backslash\{0\},i\neq j}\sum_{p\in P_{ij}}\tau_p+\sum_{i\in V,i\neq j}\sum_{p\in P_{ij}}\left(t^p x_p+\sum_{l\in L_p}(\Delta_{pl}+\nabla_{pl})\right)+p_j=\sum_{l\in\tilde{V},l\neq j}\sum_{p\in P_{jl}}\tau_p,\quad \forall j\in I \tag{56}$$

$$\tau_p+\sum_{l\in L_p}(\Delta_{pl}+\nabla_{pl})\leqslant\left(T_{max}-t^p-p_{d(p)}-t_{d(p),0}\right)x_p,\quad \forall p\in P \tag{57}$$

$$\tau_p+t_{o(p),i(p,0)}x_p+\nabla_{p0}=s_{p0},\quad \forall p\in P \tag{58}$$

$$d_{p,l-1}+t_{i(p,l-1),i(p,l)}x_p+\nabla_{pl}=s_{pl},\quad \forall p\in P,\forall l\in L_p,l\neq 0 \tag{59}$$

$$\Delta_{pl}=d_{pl}-s_{pl},\quad \forall p\in P,\forall l\in L_p \tag{60}$$

$$x_p\in\{0,1\},\quad \forall p\in P \tag{61}$$

$$\tau_p\geqslant 0, y_p\geqslant 0\quad \forall p\in P \tag{62}$$

$$q_{pl},o_{pl},s_{pl},d_{pl},\Delta_{pl},\nabla_{pl}\geqslant 0,\quad \forall p\in P,\forall l\in L_p \tag{63}$$

$$\phi_{plk}\geqslant 0\quad \forall p\in P,\forall l\in L_p,\forall k\in B_{i(p,l)}\backslash\{0\} \tag{64}$$

$$\omega_{plk}\in\{0,1\}\quad \forall p\in P,\forall l\in L_p,\forall k\in B_{i(p,l)}\backslash\{0\} \tag{65}$$

Equation (42) gives the objective of the problem: minimizing the total time (driving times, service times, and charging times). Constraints (43) ensure that each customer is visited once. Constraints (44) impose the flow conservation. Constraints (45) track the SoC of EVs at each customer. Constraints (46) track the SoC at the arrival at the first CS of each recharging path. Constraints (47) couple the SoC of an EV that leaves a CS to go to another CS. Constraints (48) ensure that if the EV travels between a vertex and the depot, it has sufficient energy to reach its destination. Constraints (49) couple the SoC tracking variable to the arc travel variables. Constraints (56) track the departure time at each vertex. (57) couple the time tracking variable to the arc travel variables, and impose the tour duration limit. Constraints (50) restrict the segments on which EVs can charge according to the state of charge they have at their arrival at CSs. Constraints (51) restrict the charging amount that can be charged on each segment. Constraints (52) impose the activation of one segment whenever an EV visit a CS. Constraints (53) are valid inequalities. Constraints (54) define the SoC of an EV after a charging operation. Constraints (55) define the time spent charging at each CS. Finally, constraints (61)–(65) define the domain of the

decision variables.

It is worth noting that other authors have proposed recharging path-based formulations for closely related problems. For instance Andelmin (2014) proposed a refueling path-based model for the G-VRP. However, his model greatly differs from ours because the author used node tracking variables and the problem contains several simplifying hypothesis: a full charging policy and a linear approximation of the charging function.

For each visit to a CS in a path of set P, we associate a charging operation $o \in O$. Every charging operation o corresponds to the visit of the CS at position l_o in a path that we denote p_o. Let O_i the set of charging operations at CS $i \in F$. Sequential binary variable $u_{oo'}$ is equal to 1 if and only if charging operation o' is constrained to start after the completion of charging operation at o. For every CS $i \in F$, we denote ε_i^+ and ε_i^- be two dummy charging operations (acting as the source and the sink of the flow). Let $(o, o') \in \left(O_i \cup \{\varepsilon_i^+\}\right) \times \left(O_i \cup \{\varepsilon_i^-\}\right)$ be a couple of charging operations, continuous flow variable $f_{oo'}$ denotes the quantity of resource that is transferred from charging operation o to charging operation o'. For notational convenience, we define $\widetilde{C}_o := 1$ for all $o \in O_i$ and $\widetilde{C}_{\varepsilon_i^+} := \widetilde{C}_{\varepsilon_i^-} := C_i$. A flow-based formulation of the capacity constraints for $[P^{path}]$ is as follows:

$$\sum_{o' \in O_i \cup \{\varepsilon_i^+\}} f_{o'o} = x_{p_o} \qquad \forall i \in F, \forall o \in O_i \tag{66}$$

$$\sum_{o' \in O_i \cup \{\varepsilon_i^+\}} f_{o'o} - \sum_{o' \in O_i \cup \{\varepsilon_i^-\}} f_{oo'} = 0, \qquad \forall i \in F, \forall o \in O_i \tag{67}$$

$$C_i - \sum_{o \in O_i \cup \{\varepsilon_i^-\}} f_{\varepsilon_i^+, o} = 0, \qquad \forall i \in F \tag{68}$$

$$\sum_{o \in O_i \cup \{\varepsilon_i^+\}} f_{o, \varepsilon_i^-} - C_i = 0, \qquad \forall i \in F \tag{69}$$

$$s_{p_o, l_o} - d_{p_{o'}, l_{o'}} \geqslant T_{max}\left(u_{o'o} - 1\right), \qquad \forall i \in F, \forall o, o' \in O_i \tag{70}$$

$$f_{oo'} \leqslant \min(\widetilde{C}_o, \widetilde{C}_o) u_{oo'}, \qquad \forall i \in F, \forall (o, o') \in \left(O_i \cup \{\varepsilon_i^+\}\right) \times \left(O_i \cup \{\varepsilon_i^-\}\right) \tag{71}$$

$$u_{oo'} \in \{0, 1\}, \qquad \forall i \in F, \forall o, o' \in O_i \tag{72}$$

$$f_{oo'} \geqslant 0 \qquad \forall i \in F, \forall (o, o') \in \left(O_i \cup \{\varepsilon_i^+\}\right) \times \left(O_i \cup \{\varepsilon_i^-\}\right) \tag{73}$$

Alternatively, to model the capacity constraints, an event-based formulation or one of the continuous formulations introduced by Kopanos et al. (2014) could be used. Some preliminary experiments revealed that those formulations are intractable (even for small instances) because they rely on a large number of binary variables and constraints. We therefore decided to abandon that path.

4. A two-stage solution method

It is known that directly solving MILP formulations is usually computationally intractable for medium-sized and especially for large-sized instances. The results in Froger

et al. (2017) confirm the limitation of MILP solvers to provide good-quality solutions to the E-VRP-NL in a reasonable amount of time even for small instances (up to 20 customers). To tackle the E-VRP-NL-C we propose a route-first assemble-second approach. The first stage of our matheuristic intends to build a high-quality and diverse pool Ω of routes. The second stage assembles solutions by selecting a subset of routes from the pool Ω. This two-stage method has been successfully applied to several hard vehicle routing problems (VRPs): the VRP with time windows (Alvarenga et al., 2007), the truck and trailer routing problem (Villegas et al., 2013), the Swap-Body VRP (Absi et al., 2015), the E-VRP-NL (Montoya et al., 2017). Traditionally, the second phase builds the best possible solution by solving a set partitioning (SP) model over the pool of routes. Route-first, assemble-second approaches have been mostly applied to problems without *route coupling constraints*. The latter means that in those problems the feasibility of one route is totally independent of the feasibility of other routes. Due to the CS capacity constraints, clearly the E-VRP-NL does not fall into this category. To the best of our knowledge, only two studies have dealt with RFAS approaches for VRPs with route coupling constraints: Morais et al. (2014) and Grangier et al. (2017) as an intensification phase of a metaheuristic for the VRP with cross docking. In both cases, the cross-dock constraints are relaxed in the SP model. Each time the SP model finds a new better solution Morais et al. (2014) applied a local search to make it meet the cross-dock constraints, whereas Grangier et al. (2017) used a constraint programming model to check its feasibility.

We first propose to relax the CS capacity constraints during the first stage and to adapt the set partitioning model of the second stage to take the limited numbers of chargers at CSs into account.

4.1. First stage: an iterated local search

The first phase of the matheuristic builds a pool of routes that meet the constraints 2, 3, and 4 described in Section 2 (i.e. all the constraints that need to be satisfied for a route are satisfied, except the CS capacity constraints). To generate these routes, we use the approach proposed by Montoya et al. (2017) for the E-VRP-NL. These authors designed an *iterated local search* (ILS) initialized with a solution provided by a constructive heuristic. The metaheuristic first sequences the customers and then takes the charging decisions. Specifically, at each iteration of the local search, the method builds a giant tour by concatenating the routes in the current solution. Then, it applies a small perturbation to the tour based on a randomized double bridge operator. Afterwards, it applies a splitting procedure to create a feasible solution to the problem. The split procedure works on an acyclic graph where nodes are customers and there exists an arc between two nodes if there exists a route where the first and the last visited customers are the origin and the tail of the arc, respectively. The procedure repairs energy-infeasible routes using a heuristic procedure that considers the insertion of one CS between each pair of customers. Solving a shortest path problem in the above graph leads to a feasible solution to the E-VRP-NL. To improve this latter, a local search is applied. This search uses two classical operators focusing on sequencing decisions: two-opt and relocate (intra-route and inter-route versions with best improvement selection). A third operator revises the charging decisions using a

MILP model. During the procedure, all the local optimum solutions are stored in a pool Ω. It is noteworthy that in all the routes in Ω do not have any waiting time (i.e. charging operations are left-shifted). Moreover, the charging decisions inside each route are already optimized.

4.2. Second stage: a decomposition method to assemble the routes

The second stage of the matheuristic builds the best possible solution from Ω. We proposed to assemble solutions using a Benders' like decomposition of the problem into a route selection master problem and a CS capacity management sub-problem. The master problem consists in selecting a set of routes such that every customer is covered exactly by one route. Every selection of routes (output of the route selection problem) yields a set of charging operations; each operation being defined by a CS, a starting time, and a recharge amount. The sub-problem checks if the CS capacity constraints can be met. We proposed three different versions of this CS capacity management sub-problem depending to the degree of freedom that we allow to modify the routes selected as a solution to the master problem. In the a first strategy, we do not revise the charging decisions (starting time and recharging amount) in the routes selection and we only check if the CS capacity constraints are satisfied for the selected routes. In the second strategy, we can delay the charging operations (i.e. postpone their starting time) to satisfy the CS capacity constraints. In other words, contrary to the first strategy, here we allow vehicles to wait for a charger if a CS is overcrowded. In the third strategy, in addition to the introduction of waiting times, we also revise the recharging amounts, but not the visited CSs.

To efficiently solve the problem while exploiting this decomposition, we adopt the following approach implemented on top of a commercial solver. We solve the SP model related to the route selection problem using a branch-and-bound algorithm. At each integer node of the branch-and-bound tree, the corresponding solution is sent to the CS capacity management problem. In the three strategies, we introduce cuts to discard infeasible selection of routes. In the two last strategies we also add cuts to account for the additional waiting times potentially introduced. Contrary to the classical implementation of Benders decomposition, we dynamically generate cuts in the branch-and-bound tree used to solve the initial relaxed master problem. More specifically, at each integer node of the branch-and-bound tree, the corresponding solution is sent to the sub-problem in order to potentially generate the Benders cuts. This method is referred to as a *Benders-based branch-and-cut* algorithm in (Naoum-Sawaya and Elhedhli, 2010) or as a *branch-and-Benders-cut method* in (Gendron et al., 2014). It also shares a lot of similarities with the *Branch&Check* framework – introduced by Thorsteinsson (2001) – and originally designed for linear and constraint programming (CP) hybridization.

In the following subsections, we provide a detailed description of our three strategies. We use the following notation. Set $\Omega_i \subseteq \Omega$ contains the routes serving customer $i \in I$ and t_r is the duration of a route $r \in \Omega$. Set $O(\Omega)$ contains all the charging operations occurring in the routes belonging to Ω and $O_i(\Omega)$ contains the charging operations occurring at CS $i \in F$. Let $\bar{\Delta}(o)$, r_o, and i_o be the duration, the route, and the CS associated with charging operation

$o \in O(\Omega)$. We define symbols $\bar{S}(o)$ and $\bar{C}(o)$ as the original starting and completion time of charging operation o in the route r_o of the pool Ω.

4.2.1. First strategy

In the first strategy, we do not revise the charging operations involved in the routes built during the ILS stage. Let us first define a MILP model for the route selection problem. We introduce binary variable x_r that is 1 if and only if route $r \in \Omega$ is selected. The MILP formulation is then the following classical SP model:

$$[HC1] \quad \min \sum_{r \in \Omega} t_r x_r \tag{74}$$

$$\sum_{r \in \Omega_i} x_r = 1, \qquad \forall i \in I \tag{75}$$

$$x_r \in \{0,1\}, \qquad \forall r \in \Omega \tag{76}$$

The objective (74) is to select the subset of routes from Ω that minimizes the total duration. Constraints (75) ensure that each customer is visited exactly once. Constraints (76) set the domain of the decision variables.

We now assume that we have a fixed selection $\Omega(\bar{x})$ of routes given by fixing the variables $\{x_r\}_{r \in \Omega}$. Specifically, we have $\Omega(\bar{x}) = \{r \in \Omega | \bar{x}_r = 1\}$. Let $SHC1(\bar{x})$ be the resulting CS capacity management problem that consists in checking the feasibility of the charging operations at every CS. $SHC1(\bar{x})$ can be decomposed into $|I|$ independent problems, one for every CS. Let define $O_i(\bar{x}) \subseteq O_i(\Omega)$ as the set of charging operations occurring at CS $i \in F$ in the routes of $\Omega(\bar{x})$. To solve $SHC1(\bar{x})$, we apply procedure *CheckCapacityCut*$(O_i(\bar{x}), C_i)$ for every CS $i \in F$ to check the existence of subsets of operations overloading the CS. If the set returned by this procedure is non-empty, there exists one or multiple time intervals during which the number of EVs charging at i is strictly greater than C_i.

To discard the current solution $\bar{x}$ in the route selection sub-problem, we add the following cuts to $[HC1]$:

$$\sum_{r \in \Psi_i(\Omega(\bar{x}), U)} x_r \leqslant C_i \qquad \forall i \in F, \forall U \in \mathcal{U} \tag{77}$$

where $\Psi_i(\Omega(\bar{x}), U) = \{r \in \Omega(\bar{x}) | O_r \cap U \neq \varnothing\}$.

These cuts simply state that the number of selected routes (according to $\bar{x}$) that have charging operations that overlap at a specific CS must be less than or equal to the number of chargers available at this CS.

We can also imagine to separate cuts for continuous solution $\bar{x}$. In that case, we check the satisfaction of the CS capacity constraints by simply considering that for every CS i every operation $o \in O_i(\bar{x})$ requires a fractional number $\bar{x}_{r_o}$ of chargers. Another strategy is to consider only the routes r such that $\bar{x}_r = 1$. In our experiments, this latter strategy proves to lead to the best results.

Procedure CheckCapacityCut(O,C)

input : - a list of charging operations L numbered from 1 to n
($L(i)$ denotes the operation at position i in the list L)
- an integer number $C \geqslant 1$ representing the maximum number of operations that can be scheduled simultaneously

output: a set containing all the maximal subsets of charging operations leading to a violation of the CS capacity constraint

```
Sort the operations in L in non-decreasing order of starting time
𝒰 ← ∅
U ← {L(1)}
k ← 2
excess ← false
while k ⩽ n do
    for every operation o ∈ U do
        if S̄(L(k)) ⩾ C̄(o) then
            if excess then
                𝒰 ← 𝒰 ∪ {U}
                excess ← false
            end
            U ← U\{o}
        end
    end
    U ← U ∪ {L(k)}
    if |𝒰| > C then
        excess ← true
    end
end
if excess then
    𝒰 ← 𝒰 ∪ {U}
end
return 𝒰
```

4.2.2. Second and third strategies

One possible drawback of the first strategy is that it may reject solutions that could be *repaired* by simply allowing the EV to wait a few minutes for a charger. As mentioned earlier, the second and third strategies consider the possibility of introducing waiting times before the charging operations. Delaying a charging operation in a route $r \in \Omega$ necessarily increases the duration of the route. Therefore, allowing the introducing of waiting times when solving the CS capacity management sub-problem may change the objective function of the solution computed when solving the route selection problem. Let θ be a non-negative variable estimating the delay added when solving the CS capacity management sub-problem.

A MILP formulation of the route selection problem (derived directly from $[HC1]$) follows:

$$[HC2] \quad \min \sum_{r\in\Omega} t_r x_r + \theta \tag{78}$$

$$\sum_{r\in\Omega_i} x_r = 1, \qquad \forall i \in I \tag{79}$$

$$\theta \geqslant 0 \tag{80}$$

$$x_r \in \{0,1\}, \qquad \forall r \in \Omega \tag{81}$$

Given a solution $\bar{x}$ of $[HC2]$, we define $\Omega(\bar{x})$ as the set of routes r selected according to $\bar{x}$ (i.e. $\Omega(\bar{x}) = \{r \in \Omega | \bar{x}_r = 1\}$). We also define $\Omega^*(\bar{x})$ as the subset of $\Omega(\bar{x})$ that contains only the routes including at least one charging operation (i.e. $\Omega^*(\bar{x}) = \{r \in \Omega(\bar{x}) | O(r) \neq \varnothing\}$). For convenience, we denote as $O(r)$ the list of charging operations occurring in route r. We assume that the operations in $O(r)$ are sorted in non-decreasing order of their starting times. We denote as $\pi^-(o)$ and $\pi^+(o)$ the charging operations preceding and following o in route r_o. If no charging operation precedes or follows before or after o, we set $\pi^-(o) = \pi^+(o) = -1$. For every route $r \in \Omega(\bar{x})$ and for each charging operation $o \in O(r)$ in a route we denote as $t^+(o)$ the travel time of the EV between the completion of o and the start of $\pi^+(o)$ if o is not the last operation of the route or the arrival at the depot. More specifically, this time corresponds to the total time spent by the vehicle covering its route between the CS associated with o and the CS associated with $pi^+(o)$ or the depot. Similarly, we define as $t^-(o)$ the time elapsed between the EV's departure from the depot (if o is the first operation of the route) or the completion of $\pi^-(o)$ and the beginning of o. We denote as $\Pi^-(o)$ and $\Pi^+(o)$ the set of charging operations preceding and following charging operation o.

Second strategy: Let $SHC2(\bar{x})$ be the problem where we want to schedule – while considering the capacity of the CSs – the charging operations occurring in the routes $\Omega(\bar{x})$ in order to minimize the addition of waiting times. Contrary to $SHC1(\bar{x})$, $SHC2(\bar{x})$ does not decompose into an independent problem for each CS. For each operation o, we introduce two parameters ES_o and LS_o representing its earliest and latest possible starting time. The parameter ES_o is equal to $\bar{S}(o)$ since by definition the operations are left shifted in each route of the pool. The parameter LS_o is computed by subtracting to T_{max} the time needed to complete the route (considering the duration of the next operations, the driving times, and no waiting times). Specifically $LS_o = T_{max} - \bar{\Delta}(o) - t^+(o) - \sum_{o'\in\Pi^+(o)}(t^+(o') + \bar{\Delta}(o'))$.

A MILP formulation of $SHC2(\bar{x})$ requires several types of decision variables. We define the continuous variable S_o defining the starting time of operation o. We model the capacity constraints using a flow-based formulation. For each CS $i \in F$, we consider two dummy operations ε_i^+ and ε_i^-, and we define $\widetilde{C}_o := 1$ for all $o \in O_i(\bar{x})$ and $\widetilde{C}_{\varepsilon_i^+} := \widetilde{C}_{\varepsilon_i^-} := C_i$. We then introduce continuous variable $f_{oo'}$ representing the quantity of resource (i.e. chargers) that is transferred from charging operation o to charging operation o'. We also define the sequential binary variable $u_{oo'}$ taking the value of 1 if operation o is processed before activity o'. A MILP formulation of $SHC2(\bar{x})$ reads:

$$[SHC2(\bar{x})] \quad \min \sum_{r\in\Omega(\bar{x})\ s.t.\ O(r)\neq\emptyset} \left(S_{o_r^{last}} - ES_{o_r^{last}}\right) \tag{82}$$

$$u_{oo'} + u_{o'o} \leqslant 1 \qquad \forall i \in F, \forall o, o' \in O_i(\bar{x}) : o < o' \tag{83}$$

$$u_{oo''} \geqslant u_{oo'} + u_{o'o''} - 1 \qquad \forall i \in F, \forall o, o', o'' \in O_i(\bar{x}) \tag{84}$$

$$S_{o'} - S_o \geqslant \bar{\Delta}(o)u_{oo'} + (LS_o - ES_{o'})(u_{oo'} - 1) \qquad \forall i \in F, \forall (o, o') \in \left(O_i(\bar{x}) \cup \{\varepsilon_i^+\}\right) \cup \left(O_i(\bar{x}) \cup \{\varepsilon_i^-\}\right) \tag{85}$$

$$S_{\pi^+(o)} - S_o \geqslant \bar{\Delta}(o) + t^+(o) \qquad \forall r \in \Omega(\bar{x}), \forall o \in O(r) : \pi^+(o) \neq -1 \tag{86}$$

$$\sum_{o'\in O_i(\bar{x})\cup\{\varepsilon_i^+\}} f_{o'o} = 1, \qquad \forall i \in F, \forall o \in O_i(\bar{x}) \tag{87}$$

$$\sum_{o'\in O_i(\bar{x})\cup\{\varepsilon_i^+\}} f_{o'o} - \sum_{o'\in O_i(\bar{x})\cup\{\varepsilon_i^-\}} f_{oo'} = 0, \qquad \forall i \in F, \forall o \in O_i(\bar{x}) \tag{88}$$

$$C_i - \sum_{o\in O_i(\bar{x})\cup\{\varepsilon_i^-\}} f_{\varepsilon_i^+,o} = 0, \qquad \forall i \in F \tag{89}$$

$$\sum_{o\in O_i(\bar{x})\cup\{\varepsilon_i^+\}} f_{o,\varepsilon_i^-} - C_i = 0, \qquad \forall i \in F \tag{90}$$

$$f_{oo'} \leqslant \max\left(\widetilde{C_o}, \widetilde{C_{o'}}\right) u_{oo'} \qquad \forall i \in F, \forall o, o' \in O_i(\bar{x}) \tag{91}$$

$$ES_o \leqslant S_o \leqslant LS_o \qquad \forall i \in F, \forall o \in O_i(\bar{x}) \tag{92}$$

$$f_{oo'} \geqslant 0 \qquad \forall i \in F, \forall (o, o') \in \left(O_i(\bar{x}) \cup \{\varepsilon_i^+\}\right) \cup \left(O_i(\bar{x}) \cup \{\varepsilon_i^-\}\right) \tag{93}$$

$$u_{oo'} \in \{0, 1\}, \qquad \forall i \in F, \forall o, o' \in O_i(\bar{x}) \tag{94}$$

The objective (82) is to minimize the waiting time inserted in each route (o_r^{last} represents the last charging operation of route r). Constraints (83) state that for two distinct operations o and o', either o precedes o', o' precedes o, or o and o' are processed in parallel. Constraints (84) express the transitivity of the precedence relations. Constraints (85) are the disjunctive constraints on the operations related to the same CS. The constraint is active when $u_{oo'} = 1$ and, in that case, it enforces the precedence relation between charging operations o and o'. Constraints (86) enforce the precedence relation and the time lag between the charging operations occurring in the same route. Constraints (87) state that a charger has to be allocated to each charging operation. Constraints (88)-(90) ensure the flow conservation. Constraints (91) couple the flow variables to the sequence variables. Constraints (92) and (94) define the domain of the decision variables.

To reduce the size of the previous model, we applied the following procedure. For every CS i and every couple of operations $(o, o') \in O_i(\bar{x})^2$, we created only the variables $u_{oo'}$ and $f_{oo'}$ if the charger used by operation o can be transferred to operation o' (i.e., $ES_o + \bar{\Delta}(o) \leqslant LS_{o'}$).

One can notice that $SHC2(\bar{x})$ is a particular parallel machine scheduling problem where the objective is to minimize the total tardiness. Indeed, one can see ES_o as the release date of each charging operation o and $ES_o + \bar{\Delta}(o)$ as its due date if o if it is the last operation of route r_o (the due date is equal to $LS_o + \bar{\Delta}(o)$ otherwise). The particularity of $SHC2(\bar{x})$ is that there is a minimum time lag between charging operations of the same route. Moreover,

the last charging operation of the route is late if it does not start exactly at its release date.

Third strategy: In addition to the introduction of waiting times, reducing congestion at CSs can come from the revision of the amounts of energy charged at each CS in every route. For example, if an EV leaves a CS i not fully charged and visits another CS j in the route, one can decide to charge more at CS i to delay the arrival of the EV at j if this latter is overcrowded. Alternatively, one can decide to charge more at CS j (if possible) to reduce the time spent at CS i. Let $(\bar{x}_r)_{r\in\Omega}$ be a fixed selection of routes (resulting in $\Omega(\bar{x})$), we denote $SHC3(\bar{x})$ the sub-problem where we want to minimize the increase in the duration of the selected routes.

We denote as $e^-(o)$ the energy consumption of the EV from its departure from i_o to its arrival at $i_{\pi^+(o)}$ if o is not the last charging operation of r_o or its arrival at the depot. This takes into account the energy consumed to visit all the customers scheduled in the route between charging operations o and $\pi^+(o)$ or the depot. Similarly, we denote as $e^+(o)$ the energy consumption of the EV from its departure from $i_{\pi^-(o)}$ if o is not the first charging operation of the route or from the depot to its arrival at i_o. Since a charging operation can be skipped by shifting energy to previous or next charging operations of the same route, we define $\widetilde{t}(o)$ and $\widetilde{e}(o)$ as the time and energy saved if the EV does not detour to perform the charging operation o.

Our modelization of $SHC3(\bar{x})$ draws very broadly on the formulation $[SHC2(\bar{x})]$. We therefore use the decision variables S_o, $f_{oo'}$, $u_{oo'}$ defined in this latter formulation. Let i be a CS. First, we introduce binary variable z_o that is 1 if and only if the charging operation $o \in O_i(\bar{x})$ is not executed anymore and the detour to the corresponding CS is not needed anymore. Specifically, z_o allows to account for special cases where shifting the charging amount to the other operations of the route can avoid charging operation o. To evaluate the impact of the revision of the charging operations, we introduce for each route $r \in \Omega^*(\bar{x})$ a continuous variable T_r that is the new duration of route r. We model the piecewise linear approximation of the charging function as in the formulation presented in Section 3. Let o be a charging operation and $k \in B_i\backslash\{0\}$. We define continuous variable ϕ_{ok} as the amount of energy charged during o on the segment that lies between the points $(c_{i,k-1}, a_{i,k-1})$ and (c_{ik}, a_{ik}) $k \in B_i$. We also define the binary variable ω_{ok} that is equal to 1 if and only if during the charging operation o the EV charges on the segment between the points $(c_{i,k-1}, a_{i,k-1})$ and (c_{ik}, a_{ik}). We introduce continuous variables y_o^1 and y_o^2 that represent the SoC of the EV before and after charging operation o. Let AE_o^{min} and AE_o^{max} be the minimum and maximum possible SoC before the beginning of o. The value of AE_o^{min} and AE_o^{max} are set considering that the EV charges the minimum (the maximum between the energy to reach the current CS and the energy needed for the detour) and maximum (the EV left the previous CS fully charged or with the energy necessary to finish the route) amount of energy at the previous CSs (if any). Similarly, let DE_o^{min} and DE_o^{max} be the minimum and maximum possible SoC after the completion of o. The value of DE_o^{min} corresponds either to the maximum between the energy to reach the next CS if any or the depot and the energy remaining after leaving the depot fully charged and visiting the previous customers and CSs in the route. The value of DE_o^{max} is the minimum between the energy that is needed to

finish the route after o and the battery capacity Q. A MILP formulation of $SHC3(\bar{x})$ reads:

$$[SHC3(\bar{x})] \quad \min \sum_{r\in\Omega(\bar{x}) \ s.t. \ O(r)\neq\varnothing} (T_r - t_r) \tag{95}$$

$$y_o^1 + \phi_{ok} \leqslant a_{ik}w_{ok} + Q(1-w_{ok}), \qquad \forall i \in F, \forall o \in O_i(\bar{x}), \forall k \in B_i\backslash\{0\} \tag{96}$$
$$\phi_{ok} \leqslant (a_{ik} - a_{i,k-1})w_{ok}, \qquad \forall i \in F, \forall o \in O_i(\bar{x}), \forall k \in B_i\backslash\{0\} \tag{97}$$
$$\sum_{k\in B_i\backslash\{0\}} w_{ok} \geqslant 1, \qquad \forall i \in F, \forall o \in O_i(\bar{x}) \tag{98}$$
$$y_o^2 = y_o^1 + \sum_{k\in B_i\backslash\{0\}} \phi_{ok}, \qquad \forall i \in F, \forall o \in O_i(\bar{x}) \tag{99}$$
$$\Delta_o = \sum_{k\in B_i\backslash\{0\}} \phi_{ok}/\rho_{ik}, \qquad \forall i \in F, \forall o \in O_i(\bar{x}) \tag{100}$$
$$\Delta_o \leqslant c_{ib_i}(1-z_o), \qquad \forall i \in F, \forall o \in O_i(\bar{x}) \tag{101}$$
$$y^1_{\pi^+(o)} = y_o^2 - e^+(o) + \widetilde{e}(o)z_o \qquad \forall r \in \Omega(\bar{x}), \forall o \in O(r), \pi^+(o) \neq -1 \tag{102}$$
$$y^2_{o_r^{last}} - e^+(o_r^{last}) + \widetilde{e}(o_r^{last})z_{o_r^{last}} \geqslant 0 \qquad \forall r \in \Omega(\bar{x}) \tag{103}$$
$$u_{oo'} + u_{o'o} \leqslant 1 \qquad \forall i \in F, \forall o, o' \in O_i(\bar{x}) : o < o' \tag{104}$$
$$u_{oo''} \geqslant u_{oo'} + u_{o'o''} - 1 \qquad \forall i \in F, \forall o, o', o'' \in O_i(\bar{x}) \tag{105}$$
$$S_{o'} - S_o \geqslant \Delta_o + (ES_{o'} - LE_o)(1-u_{oo'}) \qquad \forall i \in F, \forall o, o' \in O_i(\bar{x}) \tag{106}$$
$$S_{\pi^+(o)} - S_o \geqslant \Delta_o + t^+(o) - \widetilde{t}(o)z_o \qquad \forall r \in \Omega(\bar{x}), \forall o \in O(r), \pi^+(o) \neq -1 \tag{107}$$
$$\sum_{o'\in O_i(\bar{x})\cup\{\varepsilon_i^+\}} f_{o'o} = 1 - z_o, \qquad \forall i \in F, \forall o \in O_i(\bar{x}) \tag{108}$$
$$\sum_{o'\in O_i(\bar{x})\cup\{\varepsilon_i^+\}} f_{o'o} - \sum_{o'\in O_i(\bar{x})\cup\{\varepsilon_i^-\}} f_{oo'} = 0, \qquad \forall i \in F, \forall o \in O_i(\bar{x}) \tag{109}$$
$$C_i - \sum_{o\in O_i(\bar{x})\cup\{\varepsilon_i^-\}} f_{\varepsilon_i^+,o} = 0, \qquad \forall i \in F \tag{110}$$
$$\sum_{o\in O_i(\bar{x})\cup\{\varepsilon_i^+\}} f_{o,\varepsilon_i^-} - C_i = 0, \qquad \forall i \in F \tag{111}$$
$$f_{oo'} \leqslant \max\left(\widetilde{C_o}, \widetilde{C_{o'}}\right) u_{oo'} \qquad \forall i \in F, \forall o, o' \in O_i(\bar{x}) \tag{112}$$
$$T_r = S_{o_r^{last}} + \Delta_{o_r^{last}} - \widetilde{t}(o_r^{last}) + t^+(o_r^{last}) \qquad \forall r \in \Omega(\bar{x}), \tag{113}$$
$$T_r \leqslant T_{max} \qquad \forall r \in \Omega(\bar{x}), \tag{114}$$
$$ES_o \leqslant S_o \leqslant LE_o \qquad \forall i \in F, \forall o \in O_i(\bar{x}) \tag{115}$$
$$AE_o^{min} \leqslant y_o^1 \leqslant AE_o^{max} \qquad \forall i \in F, \forall o \in O_i(\bar{x}) \tag{116}$$
$$DE_o^{min} \leqslant y_o^2 \leqslant DE_o^{max} \qquad \forall i \in F, \forall o \in O_i(\bar{x}) \tag{117}$$
$$\phi_{ok} \geqslant 0 \qquad \forall i \in F, \forall o \in O_i(\bar{x}), \forall k \in B_i\backslash\{0\} \tag{118}$$
$$w_{ok} \in \{0,1\} \qquad \forall i \in F, \forall o \in O_i(\bar{x}), \forall k \in B_i\backslash\{0\} \tag{119}$$
$$f_{oo'} \geqslant 0 \qquad \forall i \in F, \forall (o,o') \in \left(O_i(\bar{x}) \cup \{\varepsilon_i^+\}\right) \cup \left(O_i(\bar{x}) \cup \{\varepsilon_i^-\}\right) \tag{120}$$
$$u_{oo'} \in \{0,1\}, \qquad \forall i \in F, \forall o, o' \in O_i(\bar{x}) \tag{121}$$
$$z_o \in \{0,1\}, \qquad \forall i \in F, \forall o \in O_i(\bar{x}) \tag{122}$$
$$T_r \geqslant 0, \qquad \forall r \in \Omega(\bar{x}) \tag{123}$$

The objective (95) is to minimize the additional time inserted in each route. Constraints (96)-(100) model the piecewise linear approximation of the charging function. Constraints (101) impose a duration equal to 0 for each charging operation that is removed (S_{max} is the maximum possible charging time in any CS of F). Constraints (102) couple the SoC of the EV after finishing a charging operation with its SoC when starting the next charging operation occurring in the route. Notice that if z_o is equal to 1, then the SoC $y_o^1 = y_o^2$ still takes into account the energy consumed to detour to CS i_o. The energy saved by not visiting this CS is subtracted when computing the SoC at the beginning of the next operation of the route or at the arrival at the depot (see (103)). For each route, constraints (103) enforce the corresponding EV to have enough SoC at the end of the last charging operation to reach the depot. Constraints (104), (105), and (106) define the precedence relationships between the operations. Constraints (107) enforces the precedence relation and the time lag between the charging operations occurring in the same route. Notice that if z_o is equal to 1, then the starting time S_o still takes into account the detour to CS i_o. The time saved by not visiting this CS is subtracted during the computation of the departure time for the next operation of the route or at the arrival at the depot (see (114)). Constraints (108) set if a charging operation requires a charger or not. Constraints (109) - (112) define the flow constraints. Constraints (113) compute the duration of each route. Constraints (114) enforce the tour duration limit. Constraints (115) and (122) define the domain of the decision variables.

Cut generation: The efficiency of the approach is primarily based on the constraints we generate to cut off infeasible solutions and to bound the variable θ.

When the CS capacity management sub-problem ($SHC2(\bar{x})$ or $SHC3(\bar{x})$) is infeasible, we generate an integer Benders cut, also called combinatorial Benders cuts (Codato and Fischetti, 2006) to invalidate the current solution to the restricted master problem. Let C be the set of indices of the variables x restricted to be binary and x^* the current solution to the restricted master problem. Denoting $\Omega(\bar{x}) = \{r \in \Omega | \bar{x}_r = 1\}$, a combinatorial Benders cut can be defined as follows:

$$\sum_{r \in \Omega \setminus \Omega(\bar{x})} x_r + \sum_{r \in \Omega(\bar{x})} (1 - x_r) \geqslant 1 \tag{124}$$

Clearly, this cut states that at least one of the variables of the master problem must change its value with respect to the current solution $\bar{x}$. This cut is also known as a *no-good* cut. Since every selection of routes $\bar{\Omega}$ such that $\Omega(\bar{x}) \subseteq \bar{\Omega}$ also leads to an infeasible solution, we can reformulate the cut (124) as follows:

$$\sum_{r \in \Omega(\bar{x})} x_r \leqslant |\Omega(\bar{x})| - 1 \tag{125}$$

If the sub-problem is feasible, we compare the value of θ (denoted $\bar{\theta}$) to the sub-problem objective value denoted $z^{SP}(\bar{x})$. If the objective value of the sub-problem is underestimated (i.e. $\bar{\theta} < z^{SP}(\bar{x})$), we generate integer optimality cuts to ensure that the value of the variable

θ is larger than or equal to the value of the sub-problem for the current selection of routes. Specifically, we add the following cut:

$$z^{SP}(\bar{x})\left(\sum_{r\in\Omega(\bar{x})} x_r - \sum_{r\in\Omega\setminus\Omega(\bar{x})} x_r\right) - z^{SP}(\bar{x})\left(|\Omega(\bar{x})|-1\right) + LB \leqslant \theta \tag{126}$$

These cuts are similar to those introduced by Laporte and Louveaux (1993) for the integer L-shaped method. Since every selection of routes $\bar{\Omega}$ such that $\Omega(\bar{x}) \subseteq \bar{\Omega}$ leads to a solution with a larger objective value, we can reformulate the cut (126) as follows:

$$z^{SP}(\bar{x})\left(1 + \sum_{r\in\Omega(\bar{x})} x_r - |\Omega(\bar{x})|\right) \leqslant \theta \tag{127}$$

In order to produce stronger cuts, it is noteworthy that the sub-problem may often be decomposed into several independents smaller sub-problems. Let $G(\bar{x})$ be a graph where each node represents a CS and there exists an edge between 2 CSs if there exists a route in $\Omega(\bar{x})$ with charging operations at these 2 CSs. Let $\Upsilon(G(\bar{x}))$ be the connected components of graph $G(\bar{x})$. The sub-problem can be decomposed into an independent problem for each connected component $\upsilon \in \Upsilon(G(\bar{x}))$ (where we consider only the routes with charging operations associated with CSs in υ). Let $\Omega(\bar{x},\upsilon) \subseteq \Omega(\bar{x})$ be the routes visiting the CSs that are part of υ. We can strengthen the cut (125) by replacing it by the following cuts:

$$\sum_{r\in\Omega(\bar{x},\upsilon)} x_r \leqslant |\Omega(\bar{x},\upsilon)| - 1 \quad \forall \upsilon \in \Upsilon(G(\bar{x})) \tag{128}$$

Quite similarly, we can strengthen the cut (127) by replacing it by the following cuts:

$$\left(\sum_{\upsilon\in U} z^{SP}(\bar{x},\upsilon)\right)\left(1 + \sum_{\upsilon\in U}\left(\sum_{r\in\Omega(\bar{x},\upsilon)} x_r - |\Omega(\bar{x},\upsilon)|\right)\right) \leqslant \theta \quad \forall U \in \mathcal{P}\left(\Upsilon(G(\bar{x}))\right)\setminus\{\varnothing\} \tag{129}$$

Notice that the number of these cuts can become large. In that case, we can generate the cuts (129) only for the sets U such that $|U| = 1$ or $U = \Upsilon(G(\bar{x}))$.

4.2.3. Implementation details

From an implementation point of view, we start the second stage by simply forwarding the formulation $[HC1]$ or $[HC2]$ to the MILP solver. The cut generation procedure is implemented inside a callback routine that is invoked by the solver at every node of the branch-and-bound tree. The cuts computed during this stage are provided to the solver as lazy constraints if the node is integer or as classical cuts otherwise. After adding them at a node, the solver also checks the feasibility of the solutions in terms of these constraints. If the candidate solution is not feasible, the solver discards it and adds the violated lazy constraints or cuts to the active nodes of the branch-and-bound tree.

5. Computational results

We tested the different models developed for the E-VRP-NL-C. We used Gurobi 7.0.2 to solve the ILP models through its Java API. All experiments were performed, using a single thread with 12 GB, on a cluster of 27 computers, each of which having 12 cores and two Intel(R) Xeon® X5675 3.07 GHz processors. We set a 3-hour time limit (the CPU times are reported in seconds and rounded to the nearest integer). We performed our tests on 100 instances adapted from the 120-instances testbed proposed by Montoya et al. (2017) (we adapted only the instances that contained at most 160 customers). We adapted each instance by fixing a number of chargers for each CS. We decided to consider instances in which all the CSs have the same number of chargers (1, 2, or 3). We penalized the waiting time in the objective using $K = 1$.

5.1. Mixed integer linear programming formulations

In order to assess the performance of the proposed MILP formulations, we performed our tests on small-sized instances. We restrict our tests on the 20 instances of the 120-instances testbed proposed by Montoya et al. (2017) that contains 10 customers. For CS replication-based models, the number of copies of each CS $i \in F$ is set to $\beta \in [C_i + 1, +\infty[\cap \mathbb{N}$ (i.e. $\beta_i = \beta,\ \forall i \in F$). We assume in our tests that in every instance each CS has only one charger (i.e. $C_i = 1, \forall i \in F$). Adapting the terminology used in (Froger et al., 2017), we refer to each model via "a_b_c" where a, b, and c refer to the modeling of the SoC and time tracking (A: arc-based tracking constraints), of the charging function (C: CB piecewise linear constraints / R: R piecewise linear constraints), and of the CS capacity constraints (F: flow-based / E: event-based). If the formulation uses the concept of recharging path, we add the prefix "Path". The baseline formulations $[F^{CS}]$ and $[F^{path}]$ correspond to notation "A_R" and "Path_A_R". We refer the reader to (Froger et al., 2017) for the detailed explanations of formulations "A_C" and "Path_A_C".

Table 1 present the results of the direct solution of the MILP formulations. Specifically, Table 1a and Table 1b show the results obtained when running CS-replication based and recharging path-based formulations on the MILP solver. See AppendixC for the detailed results for each instance. We report for each formulation and each value of β the number of instances optimally solved to the number of instances with a feasible solution (#Opt/#Feas), the average solution time for the instances solved to optimality (Time), and the average gap for the unsolved instances (Gap). We compute the gap $(z - z^{LB})/z$ where z is the objective of the computed solution and z^{LB} is the lower bound retrieved by the solver running the corresponding model. Moreover, since average values do not provide sufficient information, Figure 4 and Figure 5 show the number of instances optimally solved according to the solution time for all the formulations we tested.

First, we observe that, on the considered instances, the modeling of the charging function and the capacity constraints has very little impact on the results. Second, results tend to show the difficulty to optimally solve even small instances running MILP solver on CS replication-based and recharging path-based formulations. If we compare these results

Table 1: Computational results of the different models

β		A_C_E	A_C_F	A_R_E	A_R_F
2	#Opt/#Feas	15/15	15/15	15/15	15/15
	Temps (s)	486	861	131	807
3	#Opt/#Feas	18/20	18/20	19/20	17/20
	Temps (s)	764	801	1048	959
	Gap	8.6%	9.8%	7.2%	9.9%
4	#Opt/#Feas	16/20	16/20	17/20	16/20
	Temps (s)	414	719	853	764
	Gap	10.9%	13.0%	12.7%	12.8%

(a) CS-replication based formulations

	Path_A_R_F	Path_A_C_F
#Opt	14/20	16/20
Temps (s)	1468	493
Gap	15.7%	19.4%

(b) Recharging paths-based formulations

with those obtained by Froger et al. (2017) for the E-VRP-NL, the addition of the CS capacity constraints makes more complex solving the recharging-paths formulations (all the 10-customer instances are optimally solved when dropping these constraints in less than 10 minutes on average). Finally, MILP solver tends to perform slightly better on the path-based models rather than on the classical models based on the replication of the CS nodes.

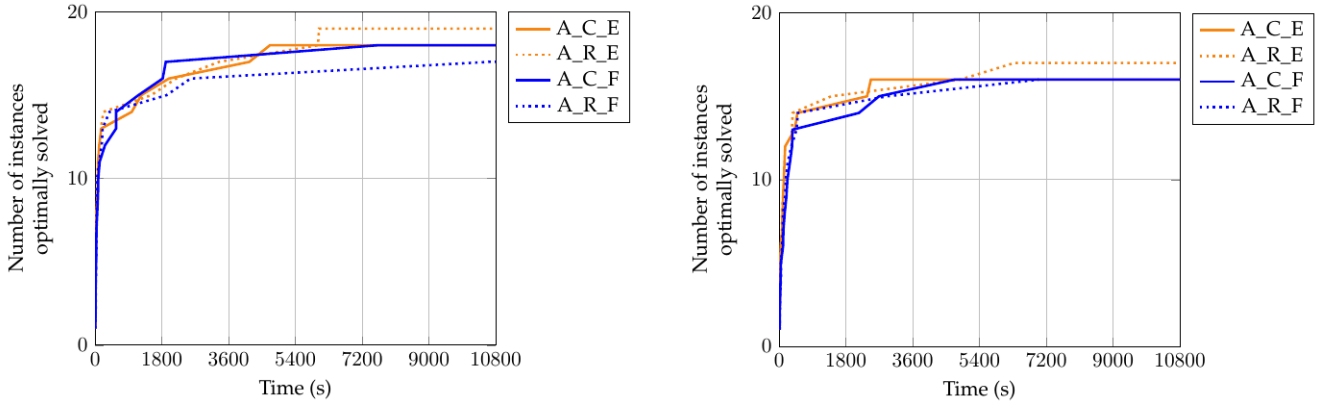

(a) $\beta = 3$ (b) $\beta = 4$

Figure 4: the different CS replication-based formulations for different values of β

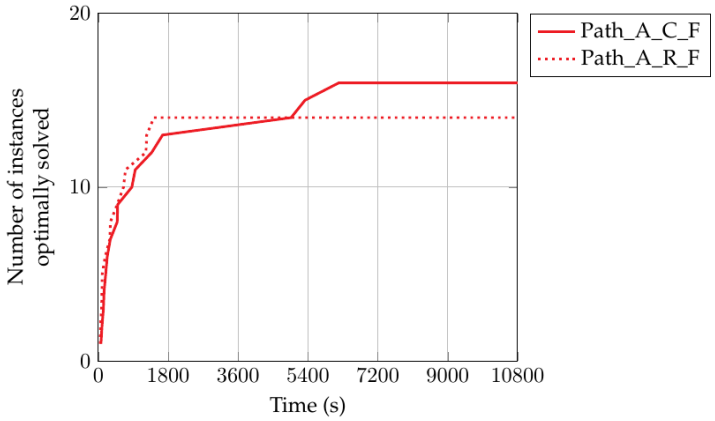

Figure 5: the different recharging path-based formulations

5.2. Two-stage algorithm

Since our contributions are solely focused on the second stage of the matheuristic, we focus our experiments only on this stage. We tested the different strategies presented in Section 4.2. For these strategies, we tested two different cutting schemes: only at every integer node (C1) or at every node[1](C2). We report in Table 2 the results obtained when using Strategy 1, Strategy 2, or Strategy 3. We also conducted another test (Strategy 4 - Post-processing) in which we solve the second stage in two steps: (1) we solve the SP model $[HC1]$ without taking the capacity constraints into account, yielding an optimal solution $\bar{x}$, and then (2) if $\bar{x}$ violates the capacity constraints, we solve the model $[SHC3(\bar{x})]$ to potentially repair it. For each value of the capacity (1, 2, and 3), we report the number of instances for which we obtained a feasible solution (#Feas), the number of best known solution reported (#BKSs), and the average solution time (Time). Notice that the solution time reported takes only the second stage of the matheuristic into account. For a meaningful comparison, we report two different gaps: the gap to the best known solutions considering only the instances for which the solution is different from the BKS (Gap*) and the gap to the BKSs considering all the instances (Gap). We also show the number of feasibility (#Cuts Feas) and optimality (#Cuts Opt) cuts generated by the algorithm.

First, if the capacity constraints are not binding, it is not very surprising to see that all the different strategies yield very similar results. We observe that Strategy 4 (and to a less extend Strategy 1) do not always provide a feasible solutions to the e-VRP-NL-C. This show the relevance of our Benders' like decomposition algorithm. Checking only the capacity constraints in a third stage could either lead to infeasibility or to worst solutions. For one instance we do not obtain a feasible solution by any of our strategies. It points out the potential need for taking the capacity constraints into account during the first stage of the algorithm. Results show that allowing delays when solving the CS capacity management sub-problem (Strategy 2 and 3) is the most suitable and efficient approach to assemble solutions in the second stage of the matheuristic. In our tests, it can be noticed that it is

[1]In the sub-problem, we only consider the routes r such that $\bar{x}_r = 1$

Table 2: Computational results according to the strategy used for the second stage of the matheuristic

Capacity		Strategy 1		Strategy 2		Strategy 3		Strategy 4
		C1	C2	C1	C2	C1	C2	Post-processing
1	#Feas	97	97	99	99	99	99	90
	#BKS	83	83	95	95	99	99	77
	Time (s)	23	20	6	5	6	5	2
	Gap	0.24%	0.24%	0.02%	0.02%	-	-	0.12%
	Gap*	1.65%	1.65%	0.41%	0.41%	-	-	0.82%
	#Cuts Feas	20.2	27.2	9.4	8.5	4	2.4	-
	#Cuts Opt	-	-	32	26	38.1	30.3	-
2	#Feas	99	99	99	99	99	99	99
	#BKS	97	97	99	99	99	99	97
	Time (s)	3	3	3	3	2	2	2
	Gap	0.01%	0.01%	-	-	-	-	0.01%
	Gap*	0.29%	0.29%	-	-	-	-	0.42%
	#Cuts Feas	0.5	0.7	0.1	0.1	0	0	-
	#Cuts Opt	-	-	0.7	0.6	0.7	0.7	-
3	#Feas	100	100	100	100	100	100	100
	#BKS	100	100	100	100	100	100	100
	Time (s)	3	2	2	3	2	2	2
	#Cuts Feas	0.1	0.1	0	0	0	0	-
	#Cuts Opt	-	-	0.3	0.3	0.3	0.3	-

not more computationally expensive than just checking the CS capacity constraints. When all CSs have a unique charger, compared to Strategy 1, using Strategy 2 and 3 improves the BKs for 12 and 14 instances out of 99, respectively. Moreover, the gap can be quite important (up to almost 15% for one instance). Last but not least, although revising the charging amounts improves only slightly the results, results show that using Strategy 3 is the best assembling method on the considered instances.

To allow future comparisons with our method, we report detailed results for each of the 120 instances in AppendixC.

6. Conclusion and perspectives

In this research, we have extended the E-VRP-NL by introducing capacity constraints at CSs. In the resulting problem (E-VRP-NL-C), the number of vehicles simultaneously charging at every CS is limited by the number of chargers.

We have introduced two modeling approaches of these constraints (flow-based and event-based). Based on this, we have proposed several CS replication-based and recharging path-based formulations of the E-VRP-NL-C. Results show that optimally solving small-sized instances is already challenging.

To tackle the E-VRP-NL-C, we have proposed a two-stage matheuristic. During the first stage, we build a set of routes using an existing metaheuristic based on iterated local search. During the second stage, we assemble these routes to build a solution to the problem using a Benders' like decomposition method. While solving the route selection problem, we consider the capacity constraints at the nodes of the branch-and-bound tree. We discard

infeasible solutions or solutions for which the objective is underestimated using cuts. We have investigated three different versions of the CS capacity management problem ranging from a simple check of the capacity constraints to the introduction of waiting times to the revision of the charging amounts in the selected routes. Results show that using more complex strategies to solve bottleneck issues at CSs does not increase on the considered instances the solution time while leading to better solutions. Results also show that the algorithm finds some optimal solutions for small-sized instances.

Future works include the revision of the first stage to include the capacity constraints and to generate routes that can be better assembled. Finally, it might be interesting to investigate if the two-stage method can provide an efficient heuristic framework to solve routing problems where dependency arise between routes.

References

Absi, N., Cattaruzza, D., Feillet, D., and Housseman, S. (2015). A relax-and-repair heuristic for the swap-body vehicle routing problem. *Annals of Operations Research*, pages 1–22.

Alvarenga, G., Mateus, G., and De Tomi, G. (2007). A genetic and set partitioning two-phase approach for the vehicle routing problem with time windows. *Computers & Operations Research*, 34(6):1561–1584.

Andelmin, J. (2014). Electric vehicle routing with realistic recharging models. Master's thesis, Aalto University, Helsinki, Finland.

Artigues, C., Michelon, P., and Reusser, S. (2003). Insertion techniques for static and dynamic resource-constrained project scheduling. *European Journal of Operational Research*, 149(2):249–267.

Bartolini, E. and Andelmin, J. (2017). An exact algorithm for the green vehicle routing problem. *Transporation Science*.

Bruglieri, M., Pezzella, F., Pisacane, O., and Suraci, S. (2015). A variable neighborhood search branching for the electric vehicle routing problem with time windows. *Electronic Notes in Discrete Mathematics*, 47:221–228.

Codato, G. and Fischetti, M. (2006). Combinatorial Benders' Cuts for Mixed-Integer Linear Programming. *Operations Research*, 54(4):756–766.

Desaulniers, G., Errico, F., Irnich, S., and Schneider, M. (2016). Exact Algorithms for Electric Vehicle-Routing Problems with Time Windows. *Operations Research*, 64(6):1388–1405.

Erdoğan, S. and Miller-Hooks, E. (2012). A green vehicle routing problem. *Transportation Research Part E: Logistics and Transportation Review*, 48(1):100–114.

Felipe, A., Ortuño, M., Righini, G., and Tirado, G. (2014). A heuristic approach for the green vehicle routing problem with multiple technologies and partial recharges. *Transportation Research Part E: Logistics and Transportation Review*, 71:111 – 128.

Froger, A., Mendoza, J., Jabali, O., and Laporte, G. (2017). New formulations for the electric vehicle routing problem with nonlinear charging function. Technical report, CIRRELT-2017-30.

Gendron, B., Scutellà, M., Garroppo, R., Nencioni, G., and Tavanti, L. (2014). A Branch-and-Benders-Cut Method for Nonlinear Power Design in Green Wireless Local Area Networks. Technical Report CIRRELT-2014-42, CIRRELT.

Grangier, P., Gendreau, M., Lehuédé, F., and Rousseau, L.-M. (2017). A matheuristic based on large neighborhood search for the vehicle routing problem with cross-docking. *Computers & Operations Research*, 84:116–126.

Hiermann, G., Puchinger, J., Ropke, S., and Hartl, R. (2016). The electric fleet size and mix vehicle routing problem with time windows and recharging stations. *European Journal of Operational Research*, 252(3):995 –1018.

Keskin, M. and Čatay, B. (2016). Partial recharge strategies for the electric vehicle routing problem with time windows. *Transportation Research Part C: Emerging Technologies*, 65:111 – 127.

Koné, O., Artigues, C., Lopez, P., and Mongeau, M. (2011). Event-based MILP models for resource-constrained project scheduling problems. *Computers & Operations Research*, 38:3–13.

Kopanos, G., Kyriakidis, T., and Georgiadis, M. (2014). New continuous-time and discrete-time mathematical formulation for resource-constrained project scheduling problems. *Computers and Chemical Engineering*, 68:96–106.

Koč, C. and Karaoglan, I. (2016). The green vehicle routing problem: A heuristic based exact solution approach. *Applied Soft Computing*, 39:154 – 164.

Laporte, G. and Louveaux, F. V. (1993). The integer l-shaped method for stochastic integer programs with complete recourse. *Operations Research Letters*, 13(3):133 – 142.

Montoya, A., Guéret, C., Mendoza, J., and Villegas, J. (2016). A multi-space sampling heuristic for the green vehicle routing problem. *Transportation Research Part C: Emerging Technologies*, 70:113–128.

Montoya, A., Guéret, C., Mendoza, J. E., and Villegas, J. G. (2017). The electric vehicle routing problem with nonlinear charging function. *Transportation Research Part B: Methodological*. 10.1016/j.trb.2017.02.004.

Morais, V., Mateus, G., and Noronha, T. (2014). Iterated local search heuristics for the vehicle routing problem with cross-docking. *Expert Systems with Applications*, 41(16):7495–7506.

Naoum-Sawaya, J. and Elhedhli, S. (2010). An interior-point Benders based branch-and-cut algorithm for mixed integer programs. *Annals of Operations Research*, 210(1):33–55.

Schneider, M., Stenger, A., and Goeke, D. (2014). The electric vehicle-routing problem with time windows and recharging stations. *Transportation Science*, 48(4):500–520.

Thorsteinsson, E. (2001). Branch-and-check: A hybrid framework integrating mixed integer programming and constraint logic programming. In Walsh, T., editor, *Principles and Practice of Constraint Programming — CP 2001*, volume 2239 of *Lecture Notes in Computer Science*, pages 16–30. Springer Berlin Heidelberg.

Villegas, J., Prins, C., Prodhon, C., Medaglia, A., and Velasco, N. (2013). A matheuristic for the truck and trailer routing problem. *European Journal of Operational Research*, 230(2):231–244.

AppendixA. Experiments on the feasibility of solutions from the literature when considering capacitated CSs

AppendixA.1. Checking the capacity constraints in a solution to the E-VRP-NL

Checking the feasibility of a solution consists in verifying that no more than C_i electric vehicles are simultaneously charged at every CS i. Let O_i be the list of charging operations occurring at CS i in the solution and C_i the number of chargers available at i. We also introduce $\bar{S}(o)$ and $\bar{C}(o)$ that define the starting time and completion time of a charging operation $o \in O_i$. The feasibility of a solution at CS i can be checked in $O(|O_i|^2)$ time by applying procedure *CheckCapacity*(O_i, C_i).

Procedure CheckCapacity(O,C)

input : - a list of charging operations L numbered from 1 to n
($L(i)$ denotes the operation at position i in the list L)
- an integer number $C \geqslant 1$ representing the maximum number of operations that can be scheduled simultaneously

output: *true* if no more than C operations overlap, *false* otherwise

```
Sort the operations in L in non-decreasing order of starting time
k ← 2
Q ← {L(1)} (Q is a set storing the operations in execution)
while k ⩽ n do
    for every operation o ∈ Q do
        if S̄(L(k)) ⩾ C̄(o) then
            Q ← Q\{o}
        end
    end
    Q ← Q ∪ {L(k)}
    if |Q| > C then
        return false
    end
    k ← k + 1
end
return true
```

AppendixA.2. Detailed results of the experiments on the best known solutions to the E-VRP-NL

Table A.3a presents the results of our experiments where we consider CSs with identical capacity. We observe that, if there exists only one charger at each CS, almost half of the solutions are infeasible. This proportion drops to 11% when considering two chargers per station, and we need to have four chargers at each CS to ensure the feasibility of all solutions. In practice, however, there are usually only one or two chargers available at each CS.

We also conducted another experiment in which we considered CSs with different capacity. We generated the number of chargers at each CS using a two-step procedure. First, we assume that the capacity of each CS independently follows a discrete uniform distribution $U(a, b)$ (we denote as ξ_i the random variable associated with the capacity of CS i). We tested different distributions: $U(1, 2)$, $U(1, 3)$, $U(1, 4)$, $U(2, 3)$, and $U(2, 4)$. Using a Monte-Carlo scheme, we then generated a sample of $n = 1000$ realizations (i.e., scenarios) of the random vector $\xi = (\xi_1, ..., \xi_{n_r})$, where n_r denotes the number of CSs in the instance. Second, we computed the proportion of realizations (in the set of all the possible realizations of ξ) for which the solution is feasible. Table A.3b shows that there is also a significant number of cases for which the solutions are infeasible even if we consider CSs with heterogenous capacity.

Experiment	$\mathcal{C}_1$	$\mathcal{C}_2$	$\mathcal{C}_3$	$\mathcal{C}_4$
Proportion of feasible solutions	54%	89%	98%	100%

(a) All CSs have the same number of chargers.

Experiment	$\mathcal{C}_{12}$	$\mathcal{C}_{13}$	$\mathcal{C}_{14}$	$\mathcal{C}_{23}$	$\mathcal{C}_{24}$
Average proportion of simulations with feasible solutions	69%	76%	81%	92%	94%

(b) The number of chargers at each CS are generated according to an uniform distribution

Table A.3: Results of the feasibility tests performed on the best solutions obtained in (Montoya et al., 2017)

AppendixB. Generation of non-dominated recharging paths

To compute the set P_{ij} for each couple of nodes $i, j \in \widetilde{V}, i \neq j$, we apply the procedure described in Algorithm 1. Let us first introduce some notation. Let p and q be a path and an initial SoC of the EV, we define function SoC_p^q that maps a duration $t \in \mathbb{R}$ to a final SoC at the destination $d(p)$. Since the charging functions we consider are piecewise linear, the function SoC_p^q also has this property. To understand the procedure, we recall the following result demonstrated in (Froger et al., 2017):

Proposition. Let $i, j \in \widetilde{V}, i \neq j$ be two nodes of the multigraph and $p, p' \in P_{ij}$ be two paths. Path p dominates path p' if $SoC_p^q(t) \geqslant SoC_{p'q}(t)$ for every $t \geqslant 0$ and for every $q \in \{e_{ij} | j \in F(i)\}$.

Using this proposition, we first fix the SoC q at the departure of i before using a label-correcting algorithm to compute all the non-dominated paths between i and j if the initial SoC is q. The underlying directed graph simply consists of a graph containing nodes i and j and every CS node. For each CS node l, we create the arcs (l, l') where l' is another CS different from l and the arcs (i, l) and (l, j). We also create the arc (i, j). The idea of the algorithm is to delay the decision about how much energy should be charge at a CS as long

as we reach j or another CS node. For this purpose, it uses SoC-functions as labels. When the EV traverses an arc, the missing energy (if there is some) is charged retroactively at the previous CS (if possible). Otherwise traversing the edge is impossible when extending the label. When we set a CS node, we create one new label for each supporting point of the current SoC-function in order to explore the possibility of switching over to the new CS at that point.

Algorithm 1: ComputeRechargingPaths(i,j)

input : two nodes $i, j \in \widetilde{V}, i \neq j$
output: a set containing all the non-dominated recharging paths between i and j

$P \leftarrow \varnothing$ (P stores the non-dominated recharging paths)
if $\left(e_{ij} + \min_{l \in F \cup \{0\}} e_{li} + \min_{l \in F \cup \{0\}} e_{jl} \leqslant Q\right)$ **then**
  $P \leftarrow P \cup \{p_{ij}^0\}$
end
for $l \in F(i)$ **do**
  Use a label-correcting algorithm to compute all the non-dominated paths with respect of an initial SoC of e_{il}.
  for each non-dominated label at j **do**
    Let p be the recharging path associated with the label
    if $p \notin P$ **then**
      $P \leftarrow P \cup \{p\}$
    end
  end
end
return P

AppendixC. Detailed computational results

We write each instance using the symbol $tc\gamma_1 c\gamma_2 s\gamma_3 c\gamma_4 \#$ where γ_1 is the method used to place the customers (i.e., 0: randomization, 1: mixture of randomization and clustering, 2: clustering), γ_2 is the number of customers, γ_3 is the number of the CSs, γ_4 is 't' if we use a p-median heuristic to locate the CSs and 'f' otherwise, and # is the number of the instance for each combination of parameters (i.e., # = 0 , 1 , 2 , 3 , 4). The symbol "Inf" means that the instance has been proven infeasible, whereas the symbol "-" means that no feasible solution has been found by the solver.

AppendixC.1. MILP formulations

Table C.4: Detailed computational results on the 10-customer instances for the CS replication-based formulations ($\beta = 2$)

Instance	A_C_E		A_R_E		A_C_F		A_R_F	
	Obj	Time	Obj	Time	Obj	Time	Obj	Time
tc0c10s2cf1	Inf	8	Inf	1	Inf	6	Inf	5
tc0c10s2ct1	17.30	17	17.30	39	17.30	12	17.30	17
tc0c10s3cf1	25.50	74	25.50	90	25.50	203	25.50	194
tc0c10s3ct1	15.80	5	15.80	4	15.80	13	15.80	18
tc1c10s2cf2	14.03	4	14.03	4	14.03	2	14.03	4
tc1c10s2cf3	Inf	24	Inf	35	Inf	47	Inf	129
tc1c10s2cf4	21.14	7	21.14	7	21.14	4	21.14	7
tc1c10s2ct2	15.75	49	15.75	53	15.75	60	15.75	42
tc1c10s2ct3	Inf	92	Inf	84	Inf	74	Inf	105
tc1c10s2ct4	18.83	7	18.83	2	18.83	6	18.83	2
tc1c10s3cf2	14.03	3	14.03	4	14.03	7	14.03	2
tc1c10s3cf3	21.94	247	21.94	141	21.94	138	21.94	64
tc1c10s3cf4	19.90	20	19.90	17	19.90	27	19.90	21
tc1c10s3ct2	14.20	64	14.20	27	14.20	103	14.20	94
tc1c10s3ct3	18.02	203	18.02	31	18.02	298	18.02	101
tc1c10s3ct4	18.21	22	18.21	9	18.21	34	18.21	14
tc2c10s2cf0	Inf	131	Inf	144	Inf	245	Inf	174
tc2c10s2ct0	18.89	993	18.89	873	18.89	1564	18.89	1553
tc2c10s3cf0	Inf	2033	Inf	2618	Inf	1298	Inf	2254
tc2c10s3ct0	16.51	5583	16.51	672	16.51	10451	16.51	9968

Table C.5: Detailed computational results on the 10-customer instances for the CS replication-based formulations ($\beta = 3$)

Instance	A_C_E		A_R_E		A_C_F		A_R_F	
	Obj	Time	Obj	Time	Obj	Time	Obj	Time
tc0c10s2cf1	24.75	27	24.75	48	24.75	87	24.75	38
tc0c10s2ct1	17.30	77	17.30	82	17.30	79	17.30	55
tc0c10s3cf1	24.75	4715	24.75	3340	24.75	1906	24.75	10800
tc0c10s3ct1	15.80	20	15.80	14	15.80	28	15.80	17
tc1c10s2cf2	14.03	12	14.03	7	14.03	7	14.03	4
tc1c10s2cf3	21.37	32	21.37	44	21.37	38	21.37	44
tc1c10s2cf4	21.10	23	21.10	14	21.10	32	21.10	48
tc1c10s2ct2	15.75	112	15.75	147	15.75	268	15.75	390
tc1c10s2ct3	18.24	15	18.24	25	18.24	16	18.24	39
tc1c10s2ct4	18.83	10	18.83	4	18.83	15	18.83	19
tc1c10s3cf2	14.03	13	14.03	6	14.03	11	14.03	21
tc1c10s3cf3	21.37	989	21.37	1513	21.37	1167	21.37	2575
tc1c10s3cf4	19.90	80	19.90	47	19.90	59	19.90	111
tc1c10s3ct2	14.20	167	14.20	155	14.20	567	14.20	182
tc1c10s3ct3	18.02	1243	18.02	226	18.02	566	18.02	201
tc1c10s3ct4	18.21	65	18.21	20	18.21	123	18.21	27
tc2c10s2cf0	27.12	4158	27.12	6038	27.12	7623	27.12	10616
tc2c10s2ct0	17.45	1990	17.45	2182	17.45	1823	17.45	1925
tc2c10s3cf0	27.12	10800	27.12	10800	27.12	10800	27.12	10800
tc2c10s3ct0	16.51	10800	16.51	6010	16.51	10800	16.51	10800

Table C.6: Detailed computational results on the 10-customer instances for the CS replication-based formulations ($\beta = 4$)

Instance	A_C_E		A_R_E		A_C_F		A_R_F	
	Obj	Time	Obj	Time	Obj	Time	Obj	Time
tc0c10s2cf1	24.75	164	24.75	161	24.75	116	24.75	228
tc0c10s2ct1	17.30	90	17.30	269	17.30	106	17.30	164
tc0c10s3cf1	24.75	10800	24.75	10800	24.75	10800	24.75	10800
tc0c10s3ct1	15.80	28	15.80	109	15.80	39	15.80	82
tc1c10s2cf2	14.03	10	14.03	13	14.03	15	14.03	21
tc1c10s2cf3	21.37	106	21.37	74	21.37	361	21.37	97
tc1c10s2cf4	21.10	40	21.10	23	21.10	49	21.10	106
tc1c10s2ct2	15.75	144	15.75	340	15.75	290	15.75	470
tc1c10s2ct3	18.24	25	18.24	44	18.24	151	18.24	48
tc1c10s2ct4	18.83	31	18.83	6	18.83	18	18.83	16
tc1c10s3cf2	14.03	13	14.03	15	14.03	28	14.03	27
tc1c10s3cf3	21.37	421	21.37	4881	21.37	4726	21.37	6999
tc1c10s3cf4	19.90	127	19.90	75	19.90	197	19.90	180
tc1c10s3ct2	14.20	494	14.20	366	14.20	350	14.20	329
tc1c10s3ct3	18.02	2371	18.02	345	18.02	2693	18.02	507
tc1c10s3ct4	18.21	83	18.21	44	18.21	224	18.21	50
tc2c10s2cf0	26.83	10800	26.83	10800	26.83	10800	26.83	10800
tc2c10s2ct0	17.45	2474	17.45	1402	17.45	2151	17.45	2909
tc2c10s3cf0	26.83	10800	26.83	10800	27.26	10800	26.83	10800
tc2c10s3ct0	16.51	10800	16.51	6338	16.51	10800	16.51	10800

Table C.7: Detailed computational results on the 10-customer instances for the recharging path-based formulations

Instance	Path_A_C_F		Path_A_R_F	
	Obj	Time	Obj	Time
tc0c10s2cf1	24.75	148	24.75	100
tc0c10s2ct1	17.30	951	17.30	1431
tc0c10s3cf1	24.75	190	24.75	92
tc0c10s3ct1	15.80	229	15.80	176
tc1c10s2cf2	14.03	95	14.03	54
tc1c10s2cf3	21.37	863	21.37	699
tc1c10s2cf4	21.10	1376	21.10	486
tc1c10s2ct2	15.75	5324	15.75	10800
tc1c10s2ct3	18.24	309	18.24	294
tc1c10s2ct4	18.83	131	18.83	84
tc1c10s3cf2	14.03	68	14.03	52
tc1c10s3cf3	21.37	4965	21.37	1227
tc1c10s3cf4	19.90	486	19.90	648
tc1c10s3ct2	14.20	6195	14.20	10800
tc1c10s3ct3	18.02	1655	18.02	1246
tc1c10s3ct4	18.21	499	18.21	310
tc2c10s2cf0	26.83	10800	26.83	10800
tc2c10s2ct0	17.45	10800	17.45	10800
tc2c10s3cf0	26.83	10800	26.83	10800
tc2c10s3ct0	16.51	10800	16.51	10800

AppendixC.2. Two-stage matheuristic

Table C.8: Number of routes considered during the second stage

Instance	#Routes
tc0c10s2cf1	22
tc0c10s2ct1	35
tc0c10s3cf1	22
tc0c10s3ct1	40
tc1c10s2cf2	91
tc1c10s2cf3	25
tc1c10s2cf4	42
tc1c10s2ct2	97
tc1c10s2ct3	28
tc1c10s2ct4	31
tc1c10s3cf2	91
tc1c10s3cf3	25
tc1c10s3cf4	36
tc1c10s3ct2	97
tc1c10s3ct3	45
tc1c10s3ct4	31
tc2c10s2cf0	28
tc2c10s2ct0	71
tc2c10s3cf0	28
tc2c10s3ct0	62
tc0c20s3cf2	93
tc0c20s3ct2	117
tc0c20s4cf2	110
tc0c20s4ct2	128
tc1c20s3cf1	145
tc1c20s3cf3	127
tc1c20s3cf4	95
tc1c20s3ct1	151
tc1c20s3ct3	185
tc1c20s3ct4	125
tc1c20s4cf1	156
tc1c20s4cf3	158
tc1c20s4cf4	101
tc1c20s4ct1	153
tc1c20s4ct3	125
tc1c20s4ct4	97
tc2c20s3cf0	92
tc2c20s3ct0	171
tc2c20s4cf0	110
tc2c20s4ct0	129
tc0c40s5cf0	166
tc0c40s5cf4	367
tc0c40s5ct0	127
tc0c40s5ct4	281
tc0c40s8cf0	177
tc0c40s8cf4	342
tc0c40s8ct0	146
tc0c40s8ct4	316
tc1c40s5cf1	274
tc1c40s5ct1	333
tc1c40s8cf1	233
tc1c40s8ct1	310
tc2c40s5cf2	212
tc2c40s5cf3	231
tc2c40s5ct2	224
tc2c40s5ct3	274
tc2c40s8cf2	223
tc2c40s8cf3	260
tc2c40s8ct2	255
tc2c40s8ct3	235

tc0c80s12cf0	431
tc0c80s12cf1	427
tc0c80s12ct0	442
tc0c80s12ct1	468
tc0c80s8cf0	375
tc0c80s8cf1	547
tc0c80s8ct0	385
tc0c80s8ct1	635
tc1c80s12cf2	512
tc1c80s12ct2	474
tc1c80s8cf2	506
tc1c80s8ct2	509
tc2c80s12cf3	372
tc2c80s12cf4	642
tc2c80s12ct3	373
tc2c80s12ct4	616
tc2c80s8cf3	370
tc2c80s8cf4	641
tc2c80s8ct3	335
tc2c80s8ct4	681
tc0c160s16cf2	1014
tc0c160s16cf4	1318
tc0c160s16ct2	860
tc0c160s16ct4	1254
tc0c160s24cf2	918
tc0c160s24cf4	1308
tc0c160s24ct2	953
tc0c160s24ct4	1280
tc1c160s16cf0	1282
tc1c160s16cf3	1031
tc1c160s16ct0	1277
tc1c160s16ct3	854
tc1c160s24cf0	1236
tc1c160s24cf3	1095
tc1c160s24ct0	1210
tc1c160s24ct3	974
tc2c160s16cf1	930
tc2c160s16ct1	794
tc2c160s24cf1	773
tc2c160s24ct1	855

Table C.9: Detailed computational results on the 10-customer instances for the two-stage matheuristic (Capacity = 1)

Instance	Strategy 1 (C1)		Strategy 2 (C1)		Strategy 3 (C1)		Strategy 4	
	Obj	Time (s)	Obj	Time (s)	Obj	Time (s)	Obj	Time (s)
tc0c10s2cf1	25.22	0.1	25.22	0.1	25.22	0.1	25.22	51
tc0c10s2ct1	17.30	0.1	17.30	0.1	17.30	0.1	17.30	1
tc0c10s3cf1	25.22	0.1	25.22	0.1	25.22	0.1	25.22	1
tc0c10s3ct1	15.80	0	15.80	0	15.80	0.1	15.80	2
tc1c10s2cf2	14.07	0.1	14.07	0.1	14.07	0.1	14.07	0
tc1c10s2cf3	21.37	0.1	21.37	0.2	21.37	0.1	21.37	0
tc1c10s2cf4	21.10	0.1	21.10	0.2	21.10	0.1	Inf	1
tc1c10s2ct2	15.78	0.2	15.78	0.1	15.78	0.1	15.78	0
tc1c10s2ct3	21.40	0.2	18.24	0.2	18.24	0.1	18.24	5
tc1c10s2ct4	18.85	0.2	18.85	0.2	18.85	0.2	18.85	0
tc1c10s3cf2	14.07	0.1	14.07	0.2	14.07	0.1	14.07	0
tc1c10s3cf3	21.37	0.1	21.37	0.2	21.37	0.1	21.37	0
tc1c10s3cf4	19.90	0.2	19.90	0.2	19.90	0.1	20.32	5
tc1c10s3ct2	15.62	0	15.62	0	15.62	0.1	15.62	1
tc1c10s3ct3	18.02	0.1	18.02	0.1	18.02	0.1	18.02	0
tc1c10s3ct4	18.21	0.1	18.21	0.1	18.21	0.1	18.21	0
tc2c10s2cf0	Inf	0.1	27.67	1	27.58	0.8	27.81	6

tc2c10s2ct0	17.45	0.1	17.45	0.3	17.45	0.3	17.45	2
tc2c10s3cf0	Inf	0.1	27.67	0.8	27.58	0.6	27.81	5
tc2c10s3ct0	16.54	0.1	16.54	0.1	16.54	0.1	16.54	0
tc0c20s3cf2	37.81	0.2	37.81	0.5	37.81	0.5	38.00	10
tc0c20s3ct2	27.11	0.1	27.11	0.1	27.11	0.1	27.11	1
tc0c20s4cf2	37.81	0.2	37.81	0.5	37.81	0.4	37.85	11
tc0c20s4ct2	26.99	0.1	26.99	0.1	26.99	0.1	26.99	1
tc1c20s3cf1	27.53	0.1	27.53	0.2	27.53	0.2	27.53	0
tc1c20s3cf3	26.86	0	26.86	0.1	26.86	0.2	26.86	0
tc1c20s3cf4	27.00	0.1	27.00	0.1	27.00	0.1	27.00	0
tc1c20s3ct1	29.41	0.1	29.41	0.1	29.41	0.1	29.41	0
tc1c20s3ct3	22.68	0.1	22.68	0.1	22.68	0.1	22.68	0
tc1c20s3ct4	26.25	0.1	26.25	0.1	26.25	0.2	26.25	1
tc1c20s4cf1	26.39	0.1	26.39	0.2	26.39	0.1	26.39	1
tc1c20s4cf3	26.81	0.1	26.81	0.1	26.81	0.1	26.81	0
tc1c20s4cf4	27.00	0.1	27.00	0.1	27.00	0.1	27.00	0
tc1c20s4ct1	28.25	0.1	28.25	0.1	28.25	0.1	28.25	0
tc1c20s4ct3	24.43	0.1	24.43	0.2	24.43	0.1	24.43	0
tc1c20s4ct4	27.01	0.1	27.01	0.1	27.01	0.1	27.01	0
tc2c20s3cf0	34.68	0.2	34.68	0.4	34.68	0.4	35.49	19
tc2c20s3ct0	35.80	0.1	35.80	0.3	35.80	0.3	36.39	11
tc2c20s4cf0	34.74	0.2	34.74	0.3	34.74	0.4	34.98	13
tc2c20s4ct0	36.25	0.2	36.25	6.2	36.22	6.7	36.40	8
tc0c40s5cf0	53.04	0.1	53.04	0.1	53.04	0.2	53.04	1
tc0c40s5cf4	51.24	0.1	51.24	0.1	51.24	0.1	51.24	1
tc0c40s5ct0	49.23	0.2	49.23	0.1	49.23	0.1	49.23	1
tc0c40s5ct4	48.70	0.1	48.70	0.1	48.70	0.1	48.70	1
tc0c40s8cf0	53.31	0.1	53.18	0.3	53.18	0.2	53.18	10
tc0c40s8cf4	49.25	0.1	49.25	0.1	49.25	0.1	49.29	8
tc0c40s8ct0	46.79	0.1	46.79	0.1	46.79	0.1	46.79	1
tc0c40s8ct4	49.24	0.1	49.24	0.1	49.24	0.1	49.24	1
tc1c40s5cf1	Inf	0.1	-	10800	-	10800	Inf	7
tc1c40s5ct1	72.92	0.1	72.92	0.3	72.92	0.2	72.92	1
tc1c40s8cf1	63.64	0.6	62.71	1.7	62.71	1.5	Inf	4
tc1c40s8ct1	61.62	0.3	61.46	1.4	61.46	1	Inf	4
tc2c40s5cf2	47.63	0.1	47.63	0.4	47.63	0.2	47.99	6
tc2c40s5cf3	40.20	0.1	40.20	0.3	40.20	0.2	40.20	1
tc2c40s5ct2	47.03	0.1	47.03	0.8	46.99	0.5	46.99	8
tc2c40s5ct3	43.8	0.1	43.80	0.2	43.80	0.1	43.80	0
tc2c40s8cf2	47.31	0.2	47.28	0.2	47.28	0.2	47.28	6
tc2c40s8cf3	39.70	0.1	39.70	0.1	39.70	0.1	39.70	0
tc2c40s8ct2	46.66	0.1	46.66	0.2	46.66	0.2	46.66	0
tc2c40s8ct3	42.67	0	42.67	0.1	42.67	0.1	42.67	1
tc0c80s12cf0	76.18	0.2	76.18	0.2	76.18	0.1	76.18	1
tc0c80s12cf1	85.41	0.2	85.41	0.3	85.41	0.2	85.41	8
tc0c80s12ct0	79.87	0.1	79.87	0.2	79.87	0.1	79.87	2
tc0c80s12ct1	83.42	0.1	83.42	0.2	83.42	0.1	83.42	6
tc0c80s8cf0	79.64	0.1	79.64	0.2	79.64	0.1	79.76	9
tc0c80s8cf1	85.77	0.2	85.77	0.3	85.77	0.3	85.83	22
tc0c80s8ct0	81.83	0.1	81.83	0.3	81.83	0.2	81.83	1
tc0c80s8ct1	86.69	0.2	86.69	0.3	86.69	0.3	86.72	3
tc1c80s12cf2	69.20	0.1	69.20	0.2	69.20	0.2	69.20	0
tc1c80s12ct2	70.67	0.1	70.67	0.2	70.67	0.1	70.67	0
tc1c80s8cf2	71.94	0.2	71.94	0.3	71.94	0.2	71.94	0
tc1c80s8ct2	72.49	0.2	72.49	0.2	72.49	0.2	72.49	1
tc2c80s12cf3	72.53	0.1	72.53	0.2	72.53	0.1	72.53	1
tc2c80s12cf4	85.63	0.5	85.63	1.3	85.63	0.5	Inf	13
tc2c80s12ct3	71.61	0.1	71.61	0.1	71.61	0.1	71.61	0
tc2c80s12ct4	83.70	0.4	83.70	0.4	83.70	0.4	83.82	2
tc2c80s8cf3	72.76	0.1	72.76	0.1	72.75	0.2	72.75	2
tc2c80s8cf4	90.43	0.6	90.43	0.5	90.43	0.7	Inf	1
tc2c80s8ct3	72.47	0.1	72.47	0.2	72.47	0.1	72.47	1
tc2c80s8ct4	85.83	0.3	85.83	0.4	85.83	0.3	85.83	1
tc0c160s16cf2	143.65	4	143.36	1.1	143.34	0.9	143.34	33
tc0c160s16cf4	165.72	1170.6	164.04	163.9	164.02	231.3	164.1	135

tc0c160s16ct2	143.43	0.8	143.43	1.3	143.43	1.1	143.43	2
tc0c160s16ct4	163.23	137.3	162.57	48.3	162.51	84.3	Inf	39
tc0c160s24cf2	140.59	0.8	140.59	1.4	140.59	1.3	140.59	2
tc0c160s24cf4	163.40	231.8	162.75	102	162.75	125.6	Inf	22
tc0c160s24ct2	139.84	0.5	139.84	0.5	139.84	0.4	139.85	8
tc0c160s24ct4	163.69	327.9	162.60	72.2	162.58	81.6	Inf	26
tc1c160s16cf0	162.03	88.6	160.95	12.7	160.83	7.4	160.83	86
tc1c160s16cf3	153.13	26.1	153.13	23	153.13	24.1	153.37	21
tc1c160s16ct0	159.90	18.3	159.76	3.1	159.74	2.8	159.79	46
tc1c160s16ct3	156.19	2.8	156.19	10.7	154.74	1.2	154.74	18
tc1c160s24cf0	161.20	118.6	158.80	13.9	158.66	12.1	Inf	13
tc1c160s24cf3	150.79	30.2	150.79	42.6	150.79	34	150.79	1
tc1c160s24ct0	160.26	38	159.94	24.3	159.77	22.1	159.77	39
tc1c160s24ct3	149.38	0.8	149.38	0.6	149.38	0.6	149.38	1
tc2c160s16cf1	141.06	0.6	141.06	0.4	141.06	0.5	141.14	7
tc2c160s16ct1	141.43	0.8	141.39	0.6	141.39	0.5	141.39	3
tc2c160s24cf1	141.18	0.4	141.18	0.4	141.18	0.4	141.29	5
tc2c160s24ct1	141.15	1.6	141.15	1.8	141.15	1.6	141.15	1

Table C.10: Detailed computational results on the 10-customer instances for the two-stage matheuristic (Capacity = 1)

Instance	Strategy 1 (C2)		Strategy 2 (C2)		Strategy 3 (C2)	
	Obj	Time (s)	Obj	Time (s)	Obj	Time (s)
tc0c10s2cf1	25.22	0.1	25.22	0.2	25.22	0.1
tc0c10s2ct1	17.30	0.1	17.30	0.2	17.30	0.1
tc0c10s3cf1	25.22	0.1	25.22	0.1	25.22	0.1
tc0c10s3ct1	15.80	0	15.80	0	15.80	0
tc1c10s2cf2	14.07	0.1	14.07	0.1	14.07	0.1
tc1c10s2cf3	21.37	0.1	21.37	0.2	21.37	0.1
tc1c10s2cf4	21.10	0.1	21.10	0.2	21.10	0.1
tc1c10s2ct2	15.78	0.1	15.78	0.1	15.78	0.1
tc1c10s2ct3	21.40	0.1	18.24	0.1	18.24	0.1
tc1c10s2ct4	18.85	0.1	18.85	0.1	18.85	0.1
tc1c10s3cf2	14.07	0.1	14.07	0.1	14.07	0.1
tc1c10s3cf3	21.37	0.1	21.37	0.2	21.37	0.1
tc1c10s3cf4	19.90	0.1	19.90	0.1	19.90	0.1
tc1c10s3ct2	15.62	0	15.62	0	15.62	0
tc1c10s3ct3	18.02	0.1	18.02	0.1	18.02	0.1
tc1c10s3ct4	18.21	0.1	18.21	0.2	18.21	0.1
tc2c10s2cf0	Inf	0.1	27.67	0.5	27.58	0.6
tc2c10s2ct0	17.45	0.1	17.45	0.2	17.45	0.1
tc2c10s3cf0	Inf	0.1	27.67	0.9	27.58	0.5
tc2c10s3ct0	16.54	0.1	16.54	0.1	16.54	0.1
tc0c20s3cf2	37.81	0.1	37.81	0.4	37.81	0.5
tc0c20s3ct2	27.11	0.1	27.11	0.1	27.11	0.1
tc0c20s4cf2	37.81	0.1	37.81	0.4	37.81	0.4
tc0c20s4ct2	26.99	0.1	26.99	0.1	26.99	0.1
tc1c20s3cf1	27.53	0.1	27.53	0.2	27.53	0.1
tc1c20s3cf3	26.86	0	26.86	0.2	26.86	0.1
tc1c20s3cf4	27.00	0.1	27.00	0.1	27.00	0.1
tc1c20s3ct1	29.41	0.1	29.41	0.2	29.41	0.1
tc1c20s3ct3	22.68	0.1	22.68	0.1	22.68	0.1
tc1c20s3ct4	26.25	0.1	26.25	0.1	26.25	0.1
tc1c20s4cf1	26.39	0.1	26.39	0.1	26.39	0.1
tc1c20s4cf3	26.81	0.1	26.81	0.1	26.81	0.1
tc1c20s4cf4	27.00	0.1	27.00	0.1	27.00	0.1
tc1c20s4ct1	28.25	0.1	28.25	0.1	28.25	0.1
tc1c20s4ct3	24.43	0.1	24.43	0.1	24.43	0.1
tc1c20s4ct4	27.01	0.1	27.01	0.1	27.01	0.1
tc2c20s3cf0	34.68	0.1	34.68	0.3	34.68	0.4
tc2c20s3ct0	35.80	0.1	35.80	0.3	35.80	0.3
tc2c20s4cf0	34.74	0.1	34.74	0.2	34.74	0.3

tc2c20s4ct0	36.25	0.2	36.25	4	36.22	7.1
tc0c40s5cf0	53.04	0.1	53.04	0.1	53.04	0.1
tc0c40s5cf4	51.24	0.1	51.24	0.1	51.24	0.1
tc0c40s5ct0	49.23	0.1	49.23	0.1	49.23	0.1
tc0c40s5ct4	48.70	0.1	48.70	0.2	48.70	0.1
tc0c40s8cf0	53.31	0.1	53.18	0.2	53.18	0.2
tc0c40s8cf4	49.25	0.1	49.25	0.1	49.25	0.1
tc0c40s8ct0	46.79	0.1	46.79	0.1	46.79	0.1
tc0c40s8ct4	49.24	0.1	49.24	0.1	49.24	0.1
tc1c40s5cf1	Inf	0.1	Inf	3	Inf	191.5
tc1c40s5ct1	72.92	0.1	72.92	0.2	72.92	0.2
tc1c40s8cf1	63.64	0.4	62.71	1.3	62.71	1.8
tc1c40s8ct1	61.62	0.2	61.46	0.6	61.46	0.9
tc2c40s5cf2	47.63	0.1	47.63	0.2	47.63	0.1
tc2c40s5cf3	40.20	0.1	40.20	0.1	40.20	0.2
tc2c40s5ct2	47.03	0.1	47.03	0.5	46.99	0.5
tc2c40s5ct3	43.80	0.1	43.80	0.2	43.80	0.1
tc2c40s8cf2	47.31	0.1	47.28	0.1	47.28	0.1
tc2c40s8cf3	39.70	0.1	39.70	0.3	39.70	0.1
tc2c40s8ct2	46.66	0.1	46.66	0.1	46.66	0.1
tc2c40s8ct3	42.67	0	42.67	0	42.67	0
tc0c80s12cf0	76.18	0.1	76.18	0.2	76.18	0.1
tc0c80s12cf1	85.41	0.1	85.41	0.2	85.41	0.2
tc0c80s12ct0	79.87	0.1	79.87	0.2	79.87	0.1
tc0c80s12ct1	83.42	0.1	83.42	0.1	83.42	0.1
tc0c80s8cf0	79.64	0.1	79.64	0.1	79.64	0.1
tc0c80s8cf1	85.77	0.2	85.77	0.3	85.77	0.3
tc0c80s8ct0	81.83	0.1	81.83	0.2	81.83	0.2
tc0c80s8ct1	86.69	0.2	86.69	0.3	86.69	0.2
tc1c80s12cf2	69.20	0.1	69.20	0.1	69.20	0.1
tc1c80s12ct2	70.67	0.1	70.67	0.2	70.67	0.1
tc1c80s8cf2	71.94	0.2	71.94	0.3	71.94	0.2
tc1c80s8ct2	72.49	0.2	72.49	0.2	72.49	0.2
tc2c80s12cf3	72.53	0.1	72.53	0.2	72.53	0.1
tc2c80s12cf4	85.63	0.4	85.63	1.1	85.63	0.6
tc2c80s12ct3	71.61	0.1	71.61	0.2	71.61	0.1
tc2c80s12ct4	83.70	0.3	83.70	0.3	83.70	0.3
tc2c80s8cf3	72.76	0.1	72.76	0.1	72.75	0.1
tc2c80s8cf4	90.43	0.5	90.43	0.6	90.43	0.6
tc2c80s8ct3	72.47	0.1	72.47	0.2	72.47	0.1
tc2c80s8ct4	85.83	0.3	85.83	0.4	85.83	0.3
tc0c160s16cf2	143.65	2.6	143.36	1	143.34	0.9
tc0c160s16cf4	165.72	1077.8	164.04	112	164.02	91.3
tc0c160s16ct2	143.43	0.6	143.43	1.1	143.43	1
tc0c160s16ct4	163.23	94.4	162.57	71.2	162.51	78.7
tc0c160s24cf2	140.59	0.7	140.59	1.5	140.59	1.1
tc0c160s24cf4	163.40	294.7	162.75	129.7	162.75	108.1
tc0c160s24ct2	139.84	0.4	139.84	0.5	139.84	0.4
tc0c160s24ct4	163.69	199.4	162.60	65.7	162.58	111.4
tc1c160s16cf0	162.03	71.1	160.95	10.2	160.83	7.2
tc1c160s16cf3	153.13	24.2	153.13	19.5	153.13	13.9
tc1c160s16ct0	159.90	19.3	159.76	3	159.74	2.8
tc1c160s16ct3	156.19	2.2	156.19	9.5	154.74	1.2
tc1c160s24cf0	161.20	67.4	158.80	11.4	158.66	8.5
tc1c160s24cf3	150.79	25.8	150.79	34.1	150.79	27.4
tc1c160s24ct0	160.26	28.4	159.94	14.6	159.77	18.2
tc1c160s24ct3	149.38	0.5	149.38	0.5	149.38	0.5
tc2c160s16cf1	141.06	0.5	141.06	0.4	141.06	0.4
tc2c160s16ct1	141.43	0.7	141.39	0.5	141.39	0.4
tc2c160s24cf1	141.18	0.3	141.18	0.4	141.18	0.3
tc2c160s24ct1	141.15	1.3	141.15	2.6	141.15	1.9

Table C.11: Detailed computational results on the 10-customer instances for the two-stage matheuristic (Capacity = 2)

Instance	Strategy 1 (C1)		Strategy 2 (C1)		Strategy 3 (C1)		Strategy 4	
	Obj	Time (s)	Obj	Time (s)	Obj	Time (s)	Obj	Time (s)
tc0c10s2cf1	25.22	0.1	25.22	0.1	25.22	0.1	25.22	0.1
tc0c10s2ct1	17.30	0	17.30	0	17.30	0.1	17.30	0
tc0c10s3cf1	25.22	0.1	25.22	0.1	25.22	0.1	25.22	0
tc0c10s3ct1	15.80	0	15.80	0	15.80	0.1	15.80	0
tc1c10s2cf2	14.07	0	14.07	0	14.07	0.1	14.07	0
tc1c10s2cf3	21.37	0.1	21.37	0.1	21.37	0.1	21.37	0
tc1c10s2cf4	21.10	0.1	21.10	0.1	21.10	0.1	21.10	0
tc1c10s2ct2	15.78	0.1	15.78	0.1	15.78	0.1	15.78	0
tc1c10s2ct3	18.17	0.1	18.17	0.2	18.17	0.1	18.17	0
tc1c10s2ct4	18.85	0.1	18.85	0.1	18.85	0.1	18.85	0
tc1c10s3cf2	14.07	0	14.07	0	14.07	0.1	14.07	0
tc1c10s3cf3	21.37	0.1	21.37	0.1	21.37	0.1	21.37	0
tc1c10s3cf4	19.90	0	19.90	0	19.90	0.1	19.90	0
tc1c10s3ct2	15.62	0	15.62	0	15.62	0.1	15.62	0
tc1c10s3ct3	18.02	0.1	18.02	0.2	18.02	0.1	18.02	0
tc1c10s3ct4	18.21	0	18.21	0	18.21	0.1	18.21	0
tc2c10s2cf0	26.77	0.1	26.77	0.1	26.77	0.1	26.77	0
tc2c10s2ct0	17.45	0.1	17.45	0.2	17.45	0.1	17.45	0
tc2c10s3cf0	26.77	0.1	26.77	0.1	26.77	0.1	26.77	0
tc2c10s3ct0	16.54	0.1	16.54	0	16.54	0.1	16.54	0
tc0c20s3cf2	37.60	0.1	37.60	0.1	37.60	0.1	37.60	0
tc0c20s3ct2	27.11	0	27.11	0	27.11	0.1	27.11	0
tc0c20s4cf2	37.68	0.1	37.68	0.1	37.68	0.1	37.68	0
tc0c20s4ct2	26.99	0.1	26.99	0.2	26.99	0.1	26.99	0
tc1c20s3cf1	27.53	0.2	27.53	0.1	27.53	0.1	27.53	0
tc1c20s3cf3	26.86	0	26.86	0.2	26.86	0.1	26.86	0
tc1c20s3cf4	27.00	0	27.00	0	27.00	0.10	27.00	0
tc1c20s3ct1	29.41	0.2	29.41	0.2	29.41	0.1	29.41	0
tc1c20s3ct3	22.68	0	22.68	0	22.68	0.1	22.68	0
tc1c20s3ct4	26.25	0	26.25	0	26.25	0.1	26.25	0
tc1c20s4cf1	26.39	0.1	26.39	0.2	26.39	0.1	26.39	0
tc1c20s4cf3	26.81	0.1	26.81	0.1	26.81	0.1	26.81	0
tc1c20s4cf4	27.00	0	27.00	0	27.00	0.10	27.00	0
tc1c20s4ct1	28.25	0.1	28.25	0.1	28.25	0.1	28.25	0
tc1c20s4ct3	24.43	0	24.43	0.1	24.43	0.1	24.43	0
tc1c20s4ct4	27.01	0	27.01	0	27.01	0.1	27.01	0
tc2c20s3cf0	34.68	0.1	34.68	0.4	34.68	0.4	34.88	0
tc2c20s3ct0	35.80	0.2	35.80	0.3	35.80	0.2	35.89	0
tc2c20s4cf0	34.73	0.1	34.73	0.1	34.73	0.1	34.73	0
tc2c20s4ct0	36.03	0.1	36.03	0.1	36.03	0.1	36.03	0
tc0c40s5cf0	53.04	0.2	53.04	0.1	53.04	0.1	53.04	0
tc0c40s5cf4	51.24	0.2	51.24	0.1	51.24	0.1	51.24	0
tc0c40s5ct0	49.23	0	49.23	0	49.23	0.2	49.23	0
tc0c40s5ct4	48.70	0.1	48.70	0.2	48.70	0.1	48.70	0
tc0c40s8cf0	53.14	0.1	53.14	0.2	53.14	0.1	53.14	0
tc0c40s8cf4	49.25	0.1	49.25	0.2	49.25	0.2	49.25	0
tc0c40s8ct0	46.79	0.1	46.79	0.1	46.79	0.1	46.79	0
tc0c40s8ct4	49.24	0.1	49.24	0.1	49.24	0.1	49.24	0
tc1c40s5cf1	Inf	0.2	-	10800	-	10800	Inf	0
tc1c40s5ct1	72.92	0.1	72.92	0.1	72.92	0.3	72.92	0
tc1c40s8cf1	61.59	0.1	61.59	0.2	61.59	0.3	61.59	0
tc1c40s8ct1	61.29	0.2	61.30	0.3	61.30	0.3	61.30	0.1
tc2c40s5cf2	47.60	0.1	47.60	0.1	47.60	0.1	47.60	0
tc2c40s5cf3	40.20	0.1	40.20	0.3	40.20	0.2	40.20	0
tc2c40s5ct2	46.97	0.1	46.97	0.1	46.97	0.1	46.97	0
tc2c40s5ct3	43.80	0.2	43.80	0.2	43.80	0.1	43.80	0
tc2c40s8cf2	47.19	0	47.19	0	47.19	0.1	47.19	0
tc2c40s8cf3	39.70	0.1	39.70	0.1	39.70	0.1	39.70	0
tc2c40s8ct2	46.66	0.1	46.66	0.1	46.66	0.1	46.66	0

tc2c40s8ct3	42.67	0	42.67	0	42.67	0.1	42.67	0
tc0c80s12cf0	76.18	0.1	76.18	0.1	76.18	0.2	76.18	0.1
tc0c80s12cf1	85.41	0.2	85.41	0.1	85.41	0.2	85.41	0.1
tc0c80s12ct0	79.87	0.1	79.87	0.2	79.87	0.1	79.87	0
tc0c80s12ct1	83.42	0	83.42	0	83.42	0.1	83.42	0
tc0c80s8cf0	79.64	0.1	79.64	0.2	79.64	0.1	79.64	0
tc0c80s8cf1	85.69	0.2	85.70	0.2	85.70	0.2	85.70	0.1
tc0c80s8ct0	81.83	0.1	81.83	0.2	81.83	0.1	81.83	0
tc0c80s8ct1	86.64	0.2	86.64	0.3	86.64	0.2	86.64	0.1
tc1c80s12cf2	69.20	0	69.20	0.1	69.20	0.1	69.20	0
tc1c80s12ct2	70.67	0.2	70.67	0.1	70.67	0.1	70.67	0.1
tc1c80s8cf2	71.94	0.2	71.94	0.3	71.94	0.3	71.94	0.1
tc1c80s8ct2	72.49	0.2	72.49	0.2	72.49	0.2	72.49	0.1
tc2c80s12cf3	72.53	0.1	72.53	0.2	72.53	0.1	72.53	0
tc2c80s12cf4	85.59	0.4	85.59	0.8	85.59	0.7	85.59	0.4
tc2c80s12ct3	71.61	0	71.61	0.1	71.61	0.1	71.61	0
tc2c80s12ct4	83.67	0.3	83.67	0.4	83.67	0.3	83.67	0.2
tc2c80s8cf3	72.75	0.2	72.75	0.1	72.75	0.1	72.75	0
tc2c80s8cf4	90.37	0.6	90.38	0.6	90.38	0.7	90.38	0.4
tc2c80s8ct3	72.47	0.1	72.47	0.1	72.47	0.1	72.47	0
tc2c80s8ct4	85.83	0.3	85.83	0.4	85.83	0.3	85.83	0.2
tc0c160s16cf2	143.20	0.6	143.20	0.9	143.20	0.8	143.20	0.5
tc0c160s16cf4	163.76	62.6	163.74	72.4	163.74	54.6	163.74	48.7
tc0c160s16ct2	143.43	1.1	143.43	1.4	143.43	1.2	143.43	1
tc0c160s16ct4	161.74	30.8	161.74	5.4	161.74	5.4	161.74	18
tc0c160s24cf2	140.59	0.7	140.59	1.4	140.59	1.3	140.59	0.7
tc0c160s24cf4	162.19	44.9	162.19	46.2	162.19	41.5	162.19	41.4
tc0c160s24ct2	139.83	0.4	139.83	0.3	139.83	0.4	139.83	0.3
tc0c160s24ct4	162.40	42.1	162.40	48.3	162.40	44.1	162.40	40.1
tc1c160s16cf0	160.78	25.3	160.45	2.4	160.45	2.4	160.45	1.6
tc1c160s16cf3	152.99	6.6	152.99	17.6	152.99	8.9	152.99	5.1
tc1c160s16ct0	159.73	21	159.73	7.3	159.73	6.4	159.73	18.2
tc1c160s16ct3	154.64	0.8	154.64	1.1	154.64	0.9	154.64	0.7
tc1c160s24cf0	158.36	2.4	158.36	3.8	158.36	4.1	158.41	1.9
tc1c160s24cf3	150.79	26.6	150.79	20.9	150.79	20.7	150.79	24
tc1c160s24ct0	160.26	28.4	159.71	9.9	159.66	9.1	159.66	18
tc1c160s24ct3	149.38	0.7	149.38	0.7	149.38	0.5	149.38	0.5
tc2c160s16cf1	140.94	0.5	140.94	0.6	140.94	0.4	140.94	0.3
tc2c160s16ct1	141.32	0.5	141.32	0.4	141.32	0.4	141.32	0.4
tc2c160s24cf1	141.16	0.3	141.16	0.3	141.16	0.3	141.16	0.2
tc2c160s24ct1	141.15	1.5	141.15	1.8	141.15	1.5	141.15	1.2

Table C.12: Detailed computational results on the 10-customer instances for the two-stage matheuristic (Capacity = 2)

Instance	Strategy 1 (C2)		Strategy 2 (C2)		Strategy 3 (C2)	
	Obj	Time (s)	Obj	Time (s)	Obj	Time (s)
tc0c10s2cf1	25.22	0.1	25.22	0.1	25.22	0.1
tc0c10s2ct1	17.30	0	17.30	0	17.30	0
tc0c10s3cf1	25.22	0.1	25.22	0.1	25.22	0.1
tc0c10s3ct1	15.80	0	15.80	0	15.80	0
tc1c10s2cf2	14.07	0	14.07	0	14.07	0
tc1c10s2cf3	21.37	0.1	21.37	0.1	21.37	0.1
tc1c10s2cf4	21.10	0.1	21.10	0.2	21.10	0.1
tc1c10s2ct2	15.78	0.1	15.78	0.1	15.78	0.1
tc1c10s2ct3	18.17	0.1	18.17	0.2	18.17	0.1
tc1c10s2ct4	18.85	0.1	18.85	0.1	18.85	0.1
tc1c10s3cf2	14.07	0	14.07	0	14.07	0
tc1c10s3cf3	21.37	0.1	21.37	0.1	21.37	0.1
tc1c10s3cf4	19.90	0	19.90	0	19.90	0
tc1c10s3ct2	15.62	0	15.62	0	15.62	0
tc1c10s3ct3	18.02	0.1	18.02	0.2	18.02	0.1
tc1c10s3ct4	18.21	0	18.21	0	18.21	0

tc2c10s2cf0	26.77	0.1	26.77	0.1	26.77	0.1
tc2c10s2ct0	17.45	0.1	17.45	0.1	17.45	0.1
tc2c10s3cf0	26.77	0.1	26.77	0.1	26.77	0.1
tc2c10s3ct0	16.54	0.1	16.54	0	16.54	0
tc0c20s3cf2	37.60	0.1	37.60	0.1	37.60	0.1
tc0c20s3ct2	27.11	0	27.11	0	27.11	0
tc0c20s4cf2	37.68	0.1	37.68	0.2	37.68	0.1
tc0c20s4ct2	26.99	0.1	26.99	0.1	26.99	0.1
tc1c20s3cf1	27.53	0.1	27.53	0.1	27.53	0.1
tc1c20s3cf3	26.86	0	26.86	0.1	26.86	0.1
tc1c20s3cf4	27.00	0	27.00	0	27.00	0
tc1c20s3ct1	29.41	0.1	29.41	0.1	29.41	0.1
tc1c20s3ct3	22.68	0	22.68	0	22.68	0
tc1c20s3ct4	26.25	0	26.25	0	26.25	0
tc1c20s4cf1	26.39	0.1	26.39	0.2	26.39	0.1
tc1c20s4cf3	26.81	0.1	26.81	0.1	26.81	0.1
tc1c20s4cf4	27.00	0	27.00	0	27.00	0
tc1c20s4ct1	28.25	0.1	28.25	0.2	28.25	0.1
tc1c20s4ct3	24.43	0	24.43	0	24.43	0
tc1c20s4ct4	27.01	0	27.01	0	27.01	0
tc2c20s3cf0	34.68	0.1	34.68	0.2	34.68	0.3
tc2c20s3ct0	35.80	0.1	35.80	0.2	35.80	0.1
tc2c20s4cf0	34.73	0.1	34.73	0.1	34.73	0.1
tc2c20s4ct0	36.03	0.1	36.03	0.1	36.03	0.1
tc0c40s5cf0	53.04	0.1	53.04	0.1	53.04	0.1
tc0c40s5cf4	51.24	0.1	51.24	0.1	51.24	0.1
tc0c40s5ct0	49.23	0	49.23	0	49.23	0
tc0c40s5ct4	48.70	0.1	48.70	0.1	48.70	0.1
tc0c40s8cf0	53.14	0.1	53.14	0.1	53.14	0.1
tc0c40s8cf4	49.25	0.1	49.25	0.2	49.25	0.1
tc0c40s8ct0	46.79	0.1	46.79	0.1	46.79	0.1
tc0c40s8ct4	49.24	0.1	49.24	0.1	49.24	0.1
tc1c40s5cf1	Inf	0.2	Inf	13.30	Inf	57.50
tc1c40s5ct1	72.92	0.1	72.92	0.2	72.92	0.2
tc1c40s8cf1	61.59	0.1	61.59	0.2	61.59	0.3
tc1c40s8ct1	61.29	0.1	61.30	0.2	61.30	0.3
tc2c40s5cf2	47.60	0.1	47.60	0.1	47.60	0.1
tc2c40s5cf3	40.20	0.1	40.20	0.2	40.20	0.1
tc2c40s5ct2	46.97	0.1	46.97	0.1	46.97	0.1
tc2c40s5ct3	43.80	0.1	43.80	0.2	43.80	0.1
tc2c40s8cf2	47.19	0	47.19	0	47.19	0
tc2c40s8cf3	39.70	0.1	39.70	0.1	39.70	0.1
tc2c40s8ct2	46.66	0.1	46.66	0.1	46.66	0.1
tc2c40s8ct3	42.67	0	42.67	0	42.67	0
tc0c80s12cf0	76.18	0.1	76.18	0.1	76.18	0.1
tc0c80s12cf1	85.41	0.1	85.41	0.1	85.41	0.1
tc0c80s12ct0	79.87	0.1	79.87	0.2	79.87	0.1
tc0c80s12ct1	83.42	0	83.42	0	83.42	0
tc0c80s8cf0	79.64	0.1	79.64	0.1	79.64	0.1
tc0c80s8cf1	85.69	0.2	85.70	0.2	85.70	0.2
tc0c80s8ct0	81.83	0.1	81.83	0.1	81.83	0.1
tc0c80s8ct1	86.64	0.2	86.64	0.3	86.64	0.2
tc1c80s12cf2	69.20	0	69.20	0.1	69.20	0
tc1c80s12ct2	70.67	0.1	70.67	0.2	70.67	0.1
tc1c80s8cf2	71.94	0.2	71.94	0.2	71.94	0.2
tc1c80s8ct2	72.49	0.1	72.49	0.1	72.49	0.1
tc2c80s12cf3	72.53	0.1	72.53	0.1	72.53	0.1
tc2c80s12cf4	85.59	0.4	85.59	0.8	85.59	0.6
tc2c80s12ct3	71.61	0	71.61	0.1	71.61	0
tc2c80s12ct4	83.67	0.3	83.67	0.3	83.67	0.2
tc2c80s8cf3	72.75	0.1	72.75	0.1	72.75	0.1
tc2c80s8cf4	90.37	0.5	90.38	0.7	90.38	0.6
tc2c80s8ct3	72.47	0.1	72.47	0.2	72.47	0.1
tc2c80s8ct4	85.83	0.3	85.83	0.4	85.83	0.3
tc0c160s16cf2	143.20	0.6	143.20	0.8	143.20	0.7

tc0c160s16cf4	163.76	59.5	163.74	107.8	163.74	73.6
tc0c160s16ct2	143.43	1	143.43	1.2	143.43	1.1
tc0c160s16ct4	161.74	21	161.74	7.7	161.74	6.5
tc0c160s24cf2	140.59	0.6	140.59	1.3	140.59	1.1
tc0c160s24cf4	162.19	42.2	162.19	44.6	162.19	39.8
tc0c160s24ct2	139.83	0.3	139.83	0.4	139.83	0.3
tc0c160s24ct4	162.40	48.4	162.40	48.9	162.40	43.8
tc1c160s16cf0	160.78	24.9	160.45	2.8	160.45	2.3
tc1c160s16cf3	152.99	5.6	152.99	16.9	152.99	8.9
tc1c160s16ct0	159.73	5.1	159.73	7.1	159.73	6
tc1c160s16ct3	154.64	0.7	154.64	0.8	154.64	0.7
tc1c160s24cf0	158.36	1.9	158.36	4.8	158.36	3.5
tc1c160s24cf3	150.79	24	150.79	20.5	150.79	19.5
tc1c160s24ct0	160.26	23.5	159.71	10.7	159.66	9.4
tc1c160s24ct3	149.38	0.6	149.38	0.5	149.38	0.5
tc2c160s16cf1	140.94	0.4	140.94	0.5	140.94	0.4
tc2c160s16ct1	141.32	0.4	141.32	0.4	141.32	0.3
tc2c160s24cf1	141.16	0.3	141.16	0.4	141.16	0.3
tc2c160s24ct1	141.15	1.3	141.15	1.7	141.15	1.6

Table C.13: Detailed computational results on the 10-customer instances for the two-stage matheuristic (Capacity = 3)

Instance	Strategy 1 (C1)		Strategy 2 (C1)		Strategy 3 (C1)		Strategy 4	
	Obj	Time (s)	Obj	Time (s)	Obj	Time (s)	Obj	Time (s)
tc0c10s2cf1	25.22	0	25.22	0	25.22	0.1	25.22	0.1
tc0c10s2ct1	17.30	0	17.30	0	17.30	0.2	17.30	0
tc0c10s3cf1	25.22	0	25.22	0	25.22	0.1	25.22	0
tc0c10s3ct1	15.80	0	15.80	0	15.80	0.1	15.80	0
tc1c10s2cf2	14.07	0	14.07	0	14.07	0.1	14.07	0
tc1c10s2cf3	21.37	0	21.37	0	21.37	0.1	21.37	0
tc1c10s2cf4	21.10	0	21.10	0	21.10	0.1	21.10	0
tc1c10s2ct2	15.78	0	15.78	0	15.78	0.1	15.78	0
tc1c10s2ct3	18.17	0	18.17	0	18.17	0.1	18.17	0
tc1c10s2ct4	18.85	0	18.85	0	18.85	0.1	18.85	0
tc1c10s3cf2	14.07	0	14.07	0	14.07	0.1	14.07	0
tc1c10s3cf3	21.37	0	21.37	0	21.37	0.1	21.37	0
tc1c10s3cf4	19.90	0	19.90	0	19.90	0.1	19.90	0
tc1c10s3ct2	15.62	0	15.62	0	15.62	0.1	15.62	0
tc1c10s3ct3	18.02	0	18.02	0	18.02	0.1	18.02	0
tc1c10s3ct4	18.21	0	18.21	0	18.21	0.1	18.21	0
tc2c10s2cf0	26.77	0.1	26.77	0.1	26.77	0.1	26.77	0
tc2c10s2ct0	17.45	0	17.45	0	17.45	0.1	17.45	0
tc2c10s3cf0	26.77	0.1	26.77	0.1	26.77	0.1	26.77	0
tc2c10s3ct0	16.54	0	16.54	0	16.54	0.1	16.54	0
tc0c20s3cf2	37.60	0.1	37.60	0.2	37.60	0.1	37.60	0
tc0c20s3ct2	27.11	0	27.11	0	27.11	0.1	27.11	0
tc0c20s4cf2	37.68	0.1	37.68	0.1	37.68	0.1	37.68	0
tc0c20s4ct2	26.99	0	26.99	0	26.99	0.1	26.99	0
tc1c20s3cf1	27.53	0	27.53	0	27.53	0.1	27.53	0
tc1c20s3cf3	26.86	0	26.86	0	26.86	0.1	26.86	0
tc1c20s3cf4	27.00	0	27.00	0	27.00	0.1	27.00	0
tc1c20s3ct1	29.41	0	29.41	0	29.41	0.1	29.41	0
tc1c20s3ct3	22.68	0	22.68	0	22.68	0.1	22.68	0
tc1c20s3ct4	26.25	0	26.25	0	26.25	0.1	26.25	0
tc1c20s4cf1	26.39	0.1	26.39	0.1	26.39	0.1	26.39	0
tc1c20s4cf3	26.81	0	26.81	0	26.81	0.1	26.81	0
tc1c20s4cf4	27.00	0	27.00	0	27.00	0.1	27.00	0
tc1c20s4ct1	28.25	0.1	28.25	0.2	28.25	0.1	28.25	0
tc1c20s4ct3	24.43	0	24.43	0	24.43	0.1	24.43	0
tc1c20s4ct4	27.01	0	27.01	0	27.01	0.1	27.01	0
tc2c20s3cf0	34.68	0.1	34.68	0.2	34.68	0.1	34.68	0
tc2c20s3ct0	35.80	0.2	35.80	0.2	35.80	0.1	35.80	0

tc2c20s4cf0	34.73	0.1	34.73	0.1	34.73	0.1	34.73	0
tc2c20s4ct0	36.03	0.1	36.03	0.1	36.03	0.1	36.03	0
tc0c40s5cf0	53.04	0.2	53.04	0.1	53.04	0.1	53.04	0
tc0c40s5cf4	51.24	0	51.24	0.1	51.24	0.1	51.24	0
tc0c40s5ct0	49.23	0	49.23	0	49.23	0.1	49.23	0
tc0c40s5ct4	48.70	0	48.70	0	48.70	0.1	48.70	0
tc0c40s8cf0	53.14	0	53.14	0.2	53.14	0.1	53.14	0
tc0c40s8cf4	49.25	0	49.25	0	49.25	0.1	49.25	0
tc0c40s8ct0	46.79	0	46.79	0	46.79	0.1	46.79	0
tc0c40s8ct4	49.24	0	49.24	0.1	49.24	0.2	49.24	0
tc1c40s5cf1	85.37	0.1	85.37	0.5	85.37	0.5	85.43	0.1
tc1c40s5ct1	72.92	0.1	72.92	0.1	72.92	0.1	72.92	0
tc1c40s8cf1	61.59	0.1	61.59	0.3	61.59	0.3	61.59	0
tc1c40s8ct1	61.29	0.1	61.30	0.1	61.30	0.2	61.30	0.1
tc2c40s5cf2	47.60	0	47.60	0	47.60	0.1	47.60	0
tc2c40s5cf3	40.20	0.1	40.20	0.2	40.20	0.1	40.20	0
tc2c40s5ct2	46.97	0.2	46.97	0.1	46.97	0.1	46.97	0
tc2c40s5ct3	43.80	0.1	43.80	0.2	43.80	0.1	43.80	0
tc2c40s8cf2	47.19	0	47.19	0	47.19	0.1	47.19	0
tc2c40s8cf3	39.70	0	39.70	0.1	39.70	0.1	39.70	0
tc2c40s8ct2	46.66	0.1	46.66	0.1	46.66	0.1	46.66	0
tc2c40s8ct3	42.67	0	42.67	0	42.67	0.1	42.67	0
tc0c80s12cf0	76.18	0.1	76.18	0.1	76.18	0.1	76.18	0.1
tc0c80s12cf1	85.41	0.1	85.41	0.1	85.41	0.2	85.41	0.1
tc0c80s12ct0	79.87	0.1	79.87	0.1	79.87	0.1	79.87	0
tc0c80s12ct1	83.42	0	83.42	0	83.42	0.1	83.42	0
tc0c80s8cf0	79.64	0.1	79.64	0.1	79.64	0.1	79.64	0
tc0c80s8cf1	85.69	0.2	85.70	0.2	85.70	0.2	85.70	0.1
tc0c80s8ct0	81.83	0.1	81.83	0.1	81.83	0.1	81.83	0
tc0c80s8ct1	86.64	0.1	86.64	0.2	86.64	0.3	86.64	0.1
tc1c80s12cf2	69.20	0	69.20	0.1	69.20	0.1	69.20	0
tc1c80s12ct2	70.67	0.1	70.67	0.1	70.67	0.1	70.67	0.1
tc1c80s8cf2	71.94	0.2	71.94	0.2	71.94	0.2	71.94	0.1
tc1c80s8ct2	72.49	0.1	72.49	0.2	72.49	0.2	72.49	0.1
tc2c80s12cf3	72.53	0.1	72.53	0.1	72.53	0.1	72.53	0
tc2c80s12cf4	85.59	0.5	85.59	0.8	85.59	0.7	85.59	0.4
tc2c80s12ct3	71.61	0	71.61	0	71.61	0.2	71.61	0
tc2c80s12ct4	83.67	0.3	83.67	0.4	83.67	0.3	83.67	0.2
tc2c80s8cf3	72.75	0.1	72.75	0.1	72.75	0.1	72.75	0
tc2c80s8cf4	90.37	0.5	90.38	0.6	90.38	0.6	90.38	0.4
tc2c80s8ct3	72.47	0	72.47	0	72.47	0.1	72.47	0
tc2c80s8ct4	85.83	0.3	85.83	0.3	85.83	0.3	85.83	0.2
tc0c160s16cf2	143.2	0.6	143.20	0.7	143.20	0.8	143.20	0.5
tc0c160s16cf4	163.69	52.3	163.69	46.4	163.69	42.4	163.69	48.6
tc0c160s16ct2	143.43	1.3	143.43	1.3	143.43	1.1	143.43	1
tc0c160s16ct4	161.74	20.3	161.74	5.9	161.74	5.3	161.74	18
tc0c160s24cf2	140.59	0.7	140.59	1.3	140.59	1.3	140.59	0.7
tc0c160s24cf4	162.19	44.7	162.19	76.2	162.19	73.3	162.19	41.4
tc0c160s24ct2	139.83	0.3	139.83	0.3	139.83	0.4	139.83	0.3
tc0c160s24ct4	162.4	46.9	162.40	50.3	162.40	50.2	162.40	40.1
tc1c160s16cf0	160.44	2.1	160.44	2.4	160.44	2.3	160.44	1.6
tc1c160s16cf3	152.99	6.4	152.99	10	152.99	9	152.99	5.1
tc1c160s16ct0	159.73	19	159.73	6.3	159.73	6.6	159.73	18.2
tc1c160s16ct3	154.64	0.8	154.64	0.8	154.64	0.8	154.64	0.7
tc1c160s24cf0	158.36	2.4	158.36	3.6	158.36	3	158.36	1.8
tc1c160s24cf3	150.79	27.4	150.79	22.9	150.79	20.4	150.79	24
tc1c160s24ct0	159.60	20.7	159.60	9	159.60	9.2	159.60	18
tc1c160s24ct3	149.38	0.6	149.38	0.5	149.38	0.5	149.38	0.5
tc2c160s16cf1	140.94	0.4	140.94	0.3	140.94	0.4	140.94	0.3
tc2c160s16ct1	141.32	0.4	141.32	0.3	141.32	0.4	141.32	0.4
tc2c160s24cf1	141.16	0.2	141.16	0.2	141.16	0.3	141.16	0.2
tc2c160s24ct1	141.15	1.4	141.15	1.5	141.15	1.6	141.15	1.2

Table C.14: Detailed computational results on the 10-customer instances for the two-stage matheuristic (Capacity = 3)

Instance	Strategy 1 (C2)		Strategy 2 (C2)		Strategy 3 (C2)	
	Obj	Time (s)	Obj	Time (s)	Obj	Time (s)
tc0c10s2cf1	25.22	0	25.22	0	25.22	0
tc0c10s2ct1	17.30	0	17.30	0	17.30	0
tc0c10s3cf1	25.22	0	25.22	0	25.22	0
tc0c10s3ct1	15.80	0	15.80	0	15.80	0
tc1c10s2cf2	14.07	0	14.07	0	14.07	0
tc1c10s2cf3	21.37	0	21.37	0	21.37	0
tc1c10s2cf4	21.10	0	21.10	0	21.10	0
tc1c10s2ct2	15.78	0	15.78	0	15.78	0
tc1c10s2ct3	18.17	0	18.17	0	18.17	0
tc1c10s2ct4	18.85	0	18.85	0	18.85	0
tc1c10s3cf2	14.07	0	14.07	0	14.07	0
tc1c10s3cf3	21.37	0	21.37	0	21.37	0
tc1c10s3cf4	19.90	0	19.90	0	19.90	0
tc1c10s3ct2	15.62	0	15.62	0	15.62	0
tc1c10s3ct3	18.02	0	18.02	0	18.02	0
tc1c10s3ct4	18.21	0	18.21	0	18.21	0
tc2c10s2cf0	26.77	0	26.77	0.1	26.77	0.1
tc2c10s2ct0	17.45	0	17.45	0	17.45	0
tc2c10s3cf0	26.77	0	26.77	0.1	26.77	0.1
tc2c10s3ct0	16.54	0	16.54	0	16.54	0
tc0c20s3cf2	37.60	0	37.60	0.1	37.60	0.1
tc0c20s3ct2	27.11	0	27.11	0	27.11	0
tc0c20s4cf2	37.68	0	37.68	0.1	37.68	0.1
tc0c20s4ct2	26.99	0	26.99	0	26.99	0
tc1c20s3cf1	27.53	0	27.53	0	27.53	0
tc1c20s3cf3	26.86	0	26.86	0	26.86	0
tc1c20s3cf4	27.00	0	27.00	0	27.00	0
tc1c20s3ct1	29.41	0	29.41	0	29.41	0
tc1c20s3ct3	22.68	0	22.68	0	22.68	0
tc1c20s3ct4	26.25	0	26.25	0	26.25	0
tc1c20s4cf1	26.39	0	26.39	0.1	26.39	0.1
tc1c20s4cf3	26.81	0	26.81	0	26.81	0
tc1c20s4cf4	27.00	0	27.00	0	27.00	0
tc1c20s4ct1	28.25	0	28.25	0.1	28.25	0.1
tc1c20s4ct3	24.43	0	24.43	0	24.43	0
tc1c20s4ct4	27.01	0	27.01	0	27.01	0
tc2c20s3cf0	34.68	0	34.68	0.1	34.68	0.1
tc2c20s3ct0	35.80	0	35.80	0.2	35.80	0.1
tc2c20s4cf0	34.73	0	34.73	0.1	34.73	0.1
tc2c20s4ct0	36.03	0	36.03	0.1	36.03	0.1
tc0c40s5cf0	53.04	0.1	53.04	0.1	53.04	0.1
tc0c40s5cf4	51.24	0.1	51.24	0.1	51.24	0
tc0c40s5ct0	49.23	0	49.23	0	49.23	0
tc0c40s5ct4	48.70	0	48.70	0.1	48.70	0
tc0c40s8cf0	53.14	0.1	53.14	0.1	53.14	0.1
tc0c40s8cf4	49.25	0	49.25	0	49.25	0
tc0c40s8ct0	46.79	0	46.79	0	46.79	0
tc0c40s8ct4	49.24	0	49.24	0.1	49.24	0.1
tc1c40s5cf1	85.37	0.1	85.37	0.6	85.37	0.6
tc1c40s5ct1	72.92	0.1	72.92	0.1	72.92	0.1
tc1c40s8cf1	61.59	0.1	61.59	0.3	61.59	0.2
tc1c40s8ct1	61.29	0.1	61.30	0.1	61.30	0.1
tc2c40s5cf2	47.60	0	47.60	0	47.60	0
tc2c40s5cf3	40.20	0	40.20	0.1	40.20	0.1
tc2c40s5ct2	46.97	0	46.97	0.1	46.97	0.1
tc2c40s5ct3	43.80	0	43.80	0.2	43.80	0.1
tc2c40s8cf2	47.19	0	47.19	0	47.19	0
tc2c40s8cf3	39.70	0	39.70	0.1	39.70	0.1
tc2c40s8ct2	46.66	0	46.66	0.2	46.66	0.1

tc2c40s8ct3	42.67	0	42.67	0	42.67	0
tc0c80s12cf0	76.18	0.1	76.18	0.1	76.18	0.1
tc0c80s12cf1	85.41	0.1	85.41	0.1	85.41	0.1
tc0c80s12ct0	79.87	0.1	79.87	0.1	79.87	0
tc0c80s12ct1	83.42	0.1	83.42	0	83.42	0
tc0c80s8cf0	79.64	0.1	79.64	0.1	79.64	0.1
tc0c80s8cf1	85.69	0.1	85.70	0.3	85.70	0.2
tc0c80s8ct0	81.83	0.1	81.83	0.2	81.83	0.1
tc0c80s8ct1	86.64	0.1	86.64	0.2	86.64	0.2
tc1c80s12cf2	69.20	0.1	69.20	0.1	69.20	0
tc1c80s12ct2	70.67	0.1	70.67	0.1	70.67	0
tc1c80s8cf2	71.94	0.1	71.94	0.2	71.94	0.1
tc1c80s8ct2	72.49	0.1	72.49	0.1	72.49	0.1
tc2c80s12cf3	72.53	0.1	72.53	0.1	72.53	0.1
tc2c80s12cf4	85.59	0.1	85.59	0.7	85.59	0.6
tc2c80s12ct3	71.61	0.1	71.61	0.1	71.61	0
tc2c80s12ct4	83.67	0.1	83.67	0.3	83.67	0.2
tc2c80s8cf3	72.75	0.1	72.75	0.1	72.75	0.1
tc2c80s8cf4	90.37	0.1	90.38	0.6	90.38	0.6
tc2c80s8ct3	72.47	0.1	72.47	0	72.47	0
tc2c80s8ct4	85.83	0.1	85.83	0.3	85.83	0.2
tc0c160s16cf2	143.20	0.1	143.20	0.7	143.20	0.6
tc0c160s16cf4	163.69	0.2	163.69	43	163.69	41.2
tc0c160s16ct2	143.43	0.1	143.43	1.3	143.43	1.1
tc0c160s16ct4	161.74	0.2	161.74	5.9	161.74	4.7
tc0c160s24cf2	140.59	0.1	140.59	1.3	140.59	1.1
tc0c160s24cf4	162.19	0.2	162.19	89.2	162.19	70
tc0c160s24ct2	139.83	0.1	139.83	0.3	139.83	0.3
tc0c160s24ct4	162.40	0.2	162.40	45.4	162.40	41.8
tc1c160s16cf0	160.44	0.2	160.44	2.7	160.44	2.2
tc1c160s16cf3	152.99	0.2	152.99	10.4	152.99	8.7
tc1c160s16ct0	159.73	0.2	159.73	7.1	159.73	5.8
tc1c160s16ct3	154.64	0.2	154.64	0.8	154.64	0.7
tc1c160s24cf0	158.36	0.2	158.36	3.7	158.36	2.9
tc1c160s24cf3	150.79	0.2	150.79	21.9	150.79	20.1
tc1c160s24ct0	159.60	0.2	159.60	9.8	159.60	8.5
tc1c160s24ct3	149.38	0.1	149.38	0.5	149.38	0.4
tc2c160s16cf1	140.94	0.1	140.94	0.4	140.94	0.3
tc2c160s16ct1	141.32	0.1	141.32	0.3	141.32	0.3
tc2c160s24cf1	141.16	0.1	141.16	0.2	141.16	0.2
tc2c160s24ct1	141.15	0.1	141.15	1.7	141.15	1.5